

ACCEPTED FOR PUBLICATION IN  
PLANETARY AND SPACE SCIENCE  
2010

**"Secular Light Curve of Comet  
103P/Hartley 2, target  
of the EPOXI Mission".**

Ignacio Ferrín,  
Center for Fundamental Physics,  
University of the Andes,  
Mérida 5101, VENEZUELA  
ferrin@ula.ve

Received: April 4th, 2010 , Accepted in final form Aug. 25<sup>th</sup>, 2010

Number of pages: 30+11= 41

Number of Figures: 11

Number of Tables: 2

\*The observations presented in this paper were made at the National Observatory of Venezuela (ONV), managed by the Center for Research in Astronomy (CIDA), for the Ministry of Science and Technology, (MCyT).

42  
43  
44  
45  
46  
47  
48  
49  
50  
51  
52  
53  
54  
55  
56  
57  
58  
59  
60  
61  
62  
63  
64  
65  
66  
67  
68  
69  
70  
71  
72  
73  
74  
75  
76  
77  
78  
79  
80  
81  
82  
83  
84  
85  
86  
87  
88  
89  
90  
91  
92

Proposed Running Head:

**“Secular Light Curve of Comet 103P”**

Name and address for editorial correspondence:

Dr. Ignacio Ferrín,  
Apartado 700,  
Mérida 5101-A,  
Venezuela,  
South America.

email address:

ferrin@ula.ve

93 **Abstract**

94 In support of the EPOXI mission, we have compiled and updated the secular light  
 95 curve (SLC) of comet 103P/Hartley 2, a Jupiter Family comet, the next target of the Deep  
 96 Impact extended mission. We have collected 845 observations from 1997, 121 from  
 97 1991 and 25 from 2004, and have added our own observations in 2005-2006. The main  
 98 results of this investigation are: **a)** Of the order of 30 photometric parameters are  
 99 measured and listed in the plots of this comet, over 20 of them new. Paper I (2005, Icarus  
 100 178, 493-516) gives the definitions of the parameters measured from the SLCs, although  
 101 a brief description is included here. The turn on point of activity is  $-4.2 \pm 0.1$  AU from the  
 102 Sun, which corresponds to  $-400 \pm 40$  d before perihelion. The total active time is  $T_{\text{ACTIVE}}$   
 103  $1484 \pm 43$  d. For comparison the active time of comets 1P/Halley and 9P/Tempel 1 are  
 104  $T_{\text{ACTIVE}} = 1992$  and  $1069$  days. **b)** 103P is a young dwarf comet, young because it has a  
 105 photometric age  $P\text{-AGE}(1,1) = 15 \pm 2$  cy (comet years), and dwarf because its diameter is  
 106  $D_{\text{EFFE}} = 1.14 \pm 0.16$  km. For comparison comets 1P/Halley and 9P/Tempel 1 have  
 107 photometric ages  $P\text{-AGE} = 7.1$  cy and  $P\text{-AGE} = 22$  cy (Paper V) and diameters 9.8 km and  
 108 5.5 km. **c)** The nucleus is *very active* as can be deduced from the fact that the amplitude  
 109 of the SLC is  $A_{\text{SEC}} = 10.8 \pm 0.1$  mag in 1997. For comparison comets 1P and 9P have  $A_{\text{SEC}}$   
 110  $= 10.8$  and  $9.0$  mag. Thus this comet is as active as 1P/Halley, but much smaller. **d)** This  
 111 comet belongs to the class of *spill-over* comets defined in Paper VI. After remaining  
 112 active up to aphelion, the comet spills-over its activity into the next orbit. **e)** 103P also  
 113 belongs to the family of *comets that exhibit a break point* in their SLC. Two linear laws  
 114 change slope at a break point located at  $R_{\text{BP}} = -1.20 \pm 0.1$  AU before perihelion, and  
 115 magnitude  $m_{\text{BP}} = 9.4 \pm 0.1$ . The slope of the first linear law after turn on is  $n = +9.44$ . This  
 116 value can be compared with the slope of comets Hale-Bopp, 1P/Halley and 9P/Tempel 1:  
 117  $+10.3$ ,  $+8.92$  and  $+7.7$  respectively. Since the SLC after turn on does not exhibit  
 118 curvature in any of these comets, it is safe to conclude that sublimation is not controlled by  
 119 water ice. The controlling substance may be CO or CO<sub>2</sub> ice. CO<sub>2</sub> has been detected  
 120 spectroscopically. **f)** The water budget of this comet is calculated. The comet expends  
 121  $1.88 \cdot 10^{10}$  kg of water per apparition vs  $5.5 \cdot 10^{11}$  kg for comet 1P/Halley and  $1.28 \cdot 10^{10}$  kg  
 122 for comet 9P/Tempel 1. A new water-budget age is defined and it is found that  $\text{WB-AGE}$   
 123  $= 19$  cy vs  $\text{WB-AGE} = 0.65$  cy for 1P/Halley and 28 cy for 9P. **g)** The values of  $A_{\text{fp}}$  are  
 124 calculated on two dates and we find dust production rates of 106 and 37 kg/s, decreasing  
 125 with solar distance as expected.

126

127  
128  
129  
130  
131  
132  
133  
134  
135  
136  
137  
138  
139  
140  
141  
142  
143  
144  
145  
146  
147  
148  
149  
150  
151  
152  
153  
154  
155  
156  
157  
158  
159  
160

**h)** The thickness of the layer lost per apparition is calculated, and we find  $\Delta r = 39$  m where  $r$  is the radius. Since the radius of this comet is  $r = 570$  m, it is found that at the present rate the comet may disappear in only 17 revolutions ( $\sim 109$  y). **i)** By chance all comets visited by spacecraft have small photometric ages and thus are young objects. 103P follows the same trend. Thus it is expected that the surface morphology that will be found in future EPOXI images should be very similar to that of previous comets. It is suggested that any new mission to a comet should be made to a methuselah object (P-AGE > 100 cy) and several are proposed.

## 161 1. Introduction

162 In support of the EPOXI mission (Extra-solar Planet Observation and eXtended  
163 Investigation), we have compiled and updated the secular light curve of the Jupiter family  
164 comet 103P/Hartley 2. EPOXI is the continuation of the Deep Impact mission (A'Hearn  
165 and Combi, 2007, and papers in that issue) that successfully observed the collision of an  
166 impactor with the nucleus of comet 9P/Tempel 1 (A'Hearn et al. 2005, and papers therein).

167

168 The results presented in this work parallel those of comet 9P/Tempel 1 (Ferrín,  
169 2007), thus the same parameters are derived. Since 9P/Tempel 1 was studied in depth,  
170 it may be interesting to compare the present results with the former one, to place this  
171 comet in perspective, and to predict the value of some parameters. We will present the  
172 results with a minimum of interpretation.

173

174 In Paper I (Ferrín, 2005a), we have introduced the concept of secular light curve of  
175 a comet (SLC), which includes two views, the log plot and the time plot. The SLCs  
176 provide a wealth of information on the photometric and physical properties of comets as  
177 can be deduced from subsequent works (Papers II, III, IV, V, VI, 2005b, 2006, 2007, 2008,  
178 2010), that could serve to complement other studies. In particular the *Atlas of Secular*  
179 *Light Curves of Comets* (Paper VI) is useful to get acquainted with the SLC curves, to see  
180 the rich variety of shapes exhibited by 27 comets, and to place into perspective the results  
181 presented in this paper.

182

183 Two plots are needed to characterize these objects because they provide  
184 information on different physical parameters in two different phase spaces. The  
185 importance of the time plot is that time runs uniformly in the horizontal axis, thus showing  
186 the brightness history of the object. Additionally the time plot can be converted to water  
187 production rate, allowing the calculation of the water budget of the comet (defined in  
188 Section 4). The importance of the log R plot is that power laws in R ( $R^n$ , where R= sun-  
189 comet distance), plot as straight lines, allowing the calculation of the turn on and turn off of  
190 activity. The log R plot is reflected at R=1 AU, to allow the determination of the absolute  
191 magnitude by extrapolation, thus the designation *reflected double-log R plot*.

192

193

194

195 To produce the SLCs we had to calculate ephemerides, absolute  
 196 magnitudes, separate nuclear observations, etc. A key to the photometric parameters is  
 197 given in Paper I. An updated key can be found in Paper VI. A short description is given  
 198 next.

199  
 200 The magnitude at  $\Delta$ ,  $R$ ,  $\alpha$ , is denoted by  $V(\Delta, R, \alpha)$ , where  $\Delta$  is the comet-Earth  
 201 distance,  $R$  is the Sun-comet distance, and  $\alpha$  is the phase angle. Briefly the parameters  
 202 listed in the log  $R$  plot are:  $q$ , the perihelion distance in AU,  $Q$  the aphelion distance also in  
 203 AU,  $\text{Log } Q$ , to know the extension of the plot, the turn on point  $R_{\text{ON}}$ , the turn off point  $R_{\text{OFF}}$ ,  
 204 the asymmetry parameter  $R_{\text{OFF}}/R_{\text{ON}}$ , the magnitude at turn on  $V_{\text{ON}}(1,R,0)$ , the magnitude  
 205 at turn off  $V_{\text{OFF}}(1,R,0)$ , the absolute magnitude before perihelion  $m_1(1,-1)$ , the absolute  
 206 magnitude after perihelion  $m_1(1,+1)$ , the mean value of both  $\langle m_1(1,1) \rangle$ , the value at LAG  
 207 (see definition below),  $m_1(1,\text{LAG})$ , the slope of the SLC just after turn on, the slope just  
 208 before perihelion, the slope just after perihelion, the absolute nuclear magnitude  $V_N(1,1,0)$ ,  
 209 the amplitude of the secular light curve  $A_{\text{SEC}}(1,1) = V_N(1,1,0) - \langle m_1(1,1) \rangle$ , the effective  
 210 diameter  $D_{\text{EFFE}}$ , the photometric age P-AGE(1,1) in comet years (cy), and the photometric  
 211 age calculated at LAG, P-AGE(1,LAG). In the top line of the plot, right hand side, JF13/1  
 212 means that this is a Jupiter family comet of 13 comet years of age 1 km in diameter. V.09  
 213 is the version of the plot, and Epoch indicates the year of the observations that best define  
 214 the envelope of the light curve.

215  
 216 The photometric age and the time age are defined in Papers I and II and are an  
 217 attempt to define the age of a comet through its activity:

$$219 \quad \text{P-AGE}(1,1) = 1440 / [ A_{\text{SEC}}(1,1) * (-R_{\text{ON}} + R_{\text{OFF}}) ] \text{ comet years (cy)} \quad (1)$$

$$221 \quad \text{T-AGE}(1,1) = 90240 / [ A_{\text{SEC}}(1,1) * (-T_{\text{ON}} + T_{\text{OFF}}) ] \text{ comet years (cy)} \quad (2)$$

222  
 223 where  $A_{\text{SEC}}(1,1) = V_N(1,1,0) - \langle m(1,1) \rangle$ . Thus  $A_{\text{SEC}}(1,1)$ , P-AGE(1,1) and T-AGE(1,1)  
 224 are proxies for activity and thus age and are calculated at  $\Delta = 1$  AU and  $R = 1$  AU to be  
 225 able to compare comets with different  $q$ . The validation of the concept of photometric  
 226 age, P-AGE, as a measure for age, is studied in Section 5. P-AGE has been scaled to  
 227 human years.

228

229 The time plot contains a listing of the perihelia plotted, the orbital period of the  
 230 comet,  $P_{\text{ORB}}$ , the next perihelion in format YYYYMMDD, the number of observations used  
 231 in the plot,  $N_{\text{OBS}}$ , the time lag at perihelion, LAG, the turn on time,  $T_{\text{ON}}$ , in days, the turn off  
 232 time,  $T_{\text{OFF}}$  in days, the asymmetry parameter,  $T_{\text{OFF}}/T_{\text{ON}}$ , the active time,  $T_{\text{ACTIVE}}$ , the time-  
 233 age  $T\text{-AGE}(1,1)$  in comet years (cy), the slope of the SLC at turn on,  $S_{\text{ON}}$ .

234

235 *The importance of these secular light curves is that they show not only what we*  
 236 *know, but also what we do not know, thus pointing the way to meaningful observations.*  
 237 Figures 4 and 5 show the regions where observations are missing and thus are desirable  
 238 in the next apparition. In particular observations after aphelion would determine the extent  
 239 of activity and thus  $R_{\text{OFF}}$ . It is interesting to notice that the SLCs have to be done for each  
 240 apparition. Since the comet evolves, after many apparitions it will be possible to construct  
 241 a movie of the comet in two phase spaces. *Thus each SLC is a frame of a movie.*

242

243 In this paper we have collected 840 observations in 1997, 112 in 1991 and 25 in  
 244 2004 gathered from the literature, to construct the SLCs. We will find that this Jupiter  
 245 family (JF) comet belongs to the family of *spill over comets*, those whose activity spills  
 246 over from one orbit to the next and to the family of *break point comets*, those that exhibit  
 247 a break in the power law before perihelion (Paper I). Additionally the information  
 248 presented in this study fills the important gap of photometric information and will be useful  
 249 to plan and interpret future observations of this comet.

250

## 251 **2. Photometric system**

252 The photometric system used in this work is described in Paper VI but a short  
 253 description follows.

254

255 *Envelope* No corrections were applied to the observations. The methodology outlined in  
 256 that paper makes no corrections and lets the brightest observations define the envelope.  
 257 It was found and justified there, that the *envelope* of the observations is the best  
 258 representation of the SLC of comets. The justification is that all visual observations of  
 259 comets are affected by several effects, all of which decrease the perceived brightness of  
 260 the object by washing out the outer regions of the coma: moonlight, twilight, atmospheric  
 261 absorption (low altitude), haze, cirrus clouds, dirty optics (dust on mirror), excess  
 262 magnification, large aperture, lack of collimation, excess  $f/$  number, lack of dark

263 adaptation, the delta effect, insufficient imaging exposure, insufficient measuring  
264 aperture, frame of view smaller than coma, etc. *There are no corresponding physical*  
265 *effects that could increase the perceived brightness of a comet.* Thus the envelope is the  
266 correct interpretation of the SLC and it does not require corrections of any kind. This rule  
267 is confirmed observationally. The top observations in Figure 4 show a sharp edge, while  
268 the bottom observations have no edge and are distributed in a diffuse area.

269

270 To define the envelope we follow the same procedure of Sosa and Fernandez  
271 (2009). We define 10-20 days time bins (or  $\Delta \text{Log } R = 0.1-0.2$  in the log plot), and select  
272 data points in the 5% upper percentile. These selected data points are fitted by least  
273 squares with straight lines or polynomials of up to degree 4. The fitted lines define the  
274 envelope.

275

276 *Infinite aperture magnitudes* The comet exhibited at all times a prominent coma, so no  
277 nuclear magnitude could be derived. Instead, *infinite aperture magnitudes* had to be  
278 measured (Paper II).

279

280 It has been known for some time (Green, 1997) that there is a lack of flux in many  
281 CCD observations. The reasons for this lack of flux are not always clear. Fink et al.  
282 (1999) have considered this problem and have an interesting suggestion: *"It is rather well*  
283 *known that visual observations in general, are several magnitudes brighter than CCD*  
284 *measurements and reconciling CCD visual magnitudes is "more of an art than a science".*  
285 *Figure 4 [of their work] shows why this is the case. As we increase the aperture size on*  
286 *our CCD images we get brighter magnitudes. It is evident by the progression of*  
287 *magnitudes for increasing aperture size that if we integrate farther out we would readily*  
288 *reach the magnitudes reported by visual observers. The eye is essentially a logarithmic*  
289 *detector and has a larger dynamic range than a CCD so that it effectively includes more of*  
290 *the coma than an individual non-saturated CCD exposure".*

291

292 To avoid this error we have to measure all the light from the comet. The problem  
293 can be illustrated looking at Figure 1 where we show an image of comet 103P/Hartley 2  
294 with a normal stretching of the image, and with a forced stretching. Since large  
295 photometric apertures have to be used to extract the whole flux, the image has previously  
296 been cleaned of nearby stars, using a background cloning tool. Stretching refers to the



297 maximum and minimum pixel intensity to display the image in the computer monitor.  
298 The normal stretching is selected by the computer, who does not know about preserving  
299 the flux. The computer monitor displays a deceivingly faint image. It turns out that a  
300 forced stretching reveals a much larger coma than expected (Figure 1b). Figure 1 reveals  
301 that it is all too common to use photometric CCD apertures that do not extract the whole  
302 flux from the comet. This has been called the *insufficient CCD aperture error* (Ferrín,  
303 2005b), and manifest itself by producing measurements that lie much below the envelope  
304 of the observations (see Figures 4, 5, 6). Of course the optimal extraction aperture  
305 depends on the brightness and distance of the comet.

306

307 In Figure 2 we show the method we used to extract an infinite aperture magnitude,  
308 IAM, from now on denoted as  $R_{IAM}$ ,  $V_{IAM}$ , the R and V magnitudes, respectively. The  
309 flux is measured with increasing CCD photometric apertures, and *the asymptotic value at*  
310 *infinite is the infinite aperture magnitude*. Notice how the calibration star #14 converges  
311 very rapidly to an infinite aperture magnitude. Not so the comet, that requires an aperture  
312 with more than 90 pixels in diameter to extract a total flux. Since the scale of this  
313 telescope is  $\sim 1''/\text{pixel}$ , 90 pixels represent 93" of diameter or 1.55' of diameter, clearly  
314 much larger than the usual apertures published in the literature to extract magnitudes.

315

316 Infinite aperture magnitudes should be adopted whenever the comet exhibits a  
317 coma. Currently we know only of one amateur group that carries out this type of  
318 observation on a systematic way. They are the Spanish group at  
319 <http://www.astrosurf.com/cometas-obs>. They present tables of the magnitudes of comets  
320 measured with increasing apertures. This information is enough to derive an IAM. Their  
321 work should be continued and expanded. Others groups would do well in adopting their  
322 methods of observation.

323

### 324 **3. Comet 103P/Hartley 2**

325

326 *Observations* Comet 103P/Hartley 2 was observed by the author on five nights with the  
327 1 m f/3 Schmidt telescope of the National Observatory of Venezuela over a period of over  
328 two years. The Schmidt is equipped with a mosaic camera of 4x4 CCDs of 2048x2048  
329 pixels each, for a grand total of 64 Megapixels, working in the drift scan mode. No filter  
330 was used to increase the signal to noise ratio. The maximum response curve of the CCD

331 between 6500 and 7500 Å, is approximated fairly well by a broad band R filter. The log  
332 of the observations is in Table 1.

333  
334 On January 12, 2005, 12 exposures of 142 s each were made with the 1 m Schmidt  
335 telescope. On the same night 6 exposures were obtained with the 1 m reflector, nearly  
336 simultaneously. The 1m reflector is equipped with a Tektronic CCD of 2048x2048 pixels.  
337 On January 14, 2005, 6 exposures of 300 s each were made with the 1 m reflector. The  
338 comet was re-observed on March 1<sup>st</sup>, 2006 with the 1 m Schmidt telescope, for 700 s  
339 when it was at  $R = +5.03$  AU post-perihelion and found to be fainter but still active. The  
340 comet was targeted for the last time on February 16 and 20<sup>th</sup> of 2007. On the first date 6  
341 images were combined to produce an exposure of 834 s. On the second date 13 images  
342 were combined for a total exposure of 1807 s. The comet could not be detected. We  
343 determined very carefully the limiting magnitude and we found  $m(\text{limit}) = 20.9$  for the first  
344 date and 21.3 for the second. These upper limits are not sufficient to constrain the SLC  
345 beyond  $R = +5.78$  AU,  $\Delta t = +1004$  d. Deeper images are needed at these distances. The  
346 nights were photometric. The images are shown in Figure 3.

347  
348 Processing was done using standard reduction procedures. Calibration of the  
349 magnitudes was done using the R-band magnitudes of the USNO-SA2.0 catalog. To  
350 avoid errors from poor magnitude stars, a least squares calibration of the field was done  
351 using no less than 15 stars. Stars deviating more than  $3\sigma$  from the linear fit were dropped.  
352 The magnitudes derived on January 12<sup>th</sup> of 2005 from the Schmidt and the reflector using  
353 a different focal ratio ( $f/3$  vs  $f/21$ ) differ by about +0.4 magnitudes, implying that the 21 m  
354 focal distance loses flux. It has been known for a long time that large  $f/$  ratios lose flux  
355 (Green, 1997). Using the mean color index  $\langle V-R \rangle = 0.41 \pm 0.16$  from Table 1 of Paper II,  
356 the R magnitudes were converted to visual V and are listed in Table 1. These values are  
357 plotted in the SLC, Figure 4.

358  
359 *Data sets* Observations of this comet have been collected from several sources. There  
360 are numerous observations in the International Astronomical Union Circulars (IAUC 5304,  
361 5312, 5324, 5340, 5346, 5359, 5372, 5391, 6747, 6791, 6808, 6820). Many observations  
362 come from the International Comet Quarterly (Green, 2006). The Spanish group  
363 mentioned above contributed IAM observations. Additionally the following researchers  
364 have made observations of this comet (shown in Figure 4), Chen and Jewitt (1994) = CJ,

365 Licandro et al. (2000)= LTLRH, Lowry and Fitzsimmons (2001)= LF, Lowry et al.  
366 (2003)= LFC, Groussin et al. (2004)= GLJT, Snodgrass et al. (2006)= SLF, Snodgrass et  
367 al. (2010)= SMH.

368

369 Lowry and Fitzsimmons (2001) = LF observed the comet at  $R = +3.63$  AU. Lowry et  
370 al. (2003) = LFC, have observations at  $R = +4.57$  AU. Licandro et al. (2000) = LTLRH,  
371 observed at  $R = +4.73$  AU. The largest detection distance of this author was  $R = 5.03$  AU.  
372 Chen and Jewitt (1994) = CJ, have observations of this comet at  $R = +5.12$  AU. In all  
373 those cases the comet was active. The agreement of these data sets is fairly good as can  
374 be deduced from Figures 4 and 5. But the record distance was by Snodgrass et al. (2010)  
375 at  $R = -5.492$  AU before perihelion when the comet was inactive. The observation by  
376 Snodgrass et al. (2010) made -855 days before perihelion, was critical to constrain the  
377 region of activity of the comet, and is plotted in Figures 4 and 5.

378

379 *Errors* The visual observations are affected by the insufficient flux error mentioned in  
380 Section 2. Many observations lie below the envelope so only the upper 5% is used to  
381 define the envelope as defined in Section 2.

382

383 When this series of papers was initiated, we expended many hours trying to define  
384 the envelope of the data in a mathematical way. Several algorithms were explored,  
385 including some that define edges. The envelope was also fitted independently by several  
386 students. The different fits did not differ by more than  $\pm 0.12$  magnitudes. We finally  
387 settled on the procedure followed by Sosa and Fernandez (2009) and described at the  
388 beginning of Section 2 which can define the envelope to  $\pm 0.1$  magnitudes. All the fits  
389 were made by least squares.

390

391 The professional observations have errors of 0.05 to 0.15 magnitudes. The  
392 observation of 103P on July 28<sup>th</sup>, 2008 by Snodgrass et al. (2008), has an error of  $\pm 0.20$   
393 magnitudes, but it was made at the level of magnitude 26.6, thus it is very reasonable.

394

395 In general observational errors were reasonable and comparable to those of other  
396 comets measured in this series of papers (confirmation papers I-VI).

397

398 *Nuclear and faint observations* Nuclear dimensions have been determined by  
 399 Jorda et al. (2000) who used ISOCAM of ISO, and obtained  $D = 1.16 \pm 0.2$  km. Groussin et  
 400 al. (2004) = GLJT, revised that value to  $D = 1.42 \pm 0.26$  km. Lisse et al. (2009) found  
 401  $D_{\text{NUC}} = 1.14 \pm 0.16$  km. The value by Groussin et al. (2004) was obtained +46 d after  
 402 perihelion, and thus was highly contaminated by a coma. In spite of this they did a  
 403 remarkable job of subtracting the coma. The value cited by Lisse et al. (2009) was  
 404 obtained at -5.5 AU from the Sun, and thus the coma was much less prominent, and the  
 405 diameter more near to the real value. Thus we adopt  $D_{\text{EFFE}} = 1.14 \pm 0.16$  km. Using the  
 406 classification proposed in Paper VI (*The Atlas*), we conclude that this is a *dwarf comet* ( $D$   
 407  $< 1.5$  km).

408

409 The absolute nuclear magnitude in the visual,  $V_{\text{N}}(1,1,0)$ , is related to the effective  
 410 diameter,  $D_{\text{EFFE}}$ , by a compact and amicable formula derived in Paper III:

411

$$412 \quad \text{Log} [ p_{\text{V}} D_{\text{EFFE}}^2 / 4 ] = 5.654 - 0.4 V_{\text{N}}(1,1,0)$$

413

414 where  $p_{\text{V}}$  is the geometric albedo in the visual. For comets for which the geometric  
 415 albedo has not been measured, it is common to adopt  $p_{\text{V}} = 0.04$ . Thus the previous  
 416 equation can be simplified even further:

417

$$418 \quad \text{Log} [ D_{\text{EFFE}}^2 ] = 7.654 - 0.4 V_{\text{N}}(1,1,0) \quad (3)$$

419

420 which is very easy to remember. Assuming a geometric albedo  $p_{\text{V}} = 0.04$ , then the  
 421 absolute nuclear magnitude is  $V_{\text{N}}(1,1,0) = 18.85 \pm 0.32$ .

422

423 *LAG and absolute magnitude parameters in 1997* The best observed apparition has  
 424 been that of 1997 with 840 observations. Thus most photometric parameters will be  
 425 deduced from that apparition. The comet exhibits a lag between the maximum brightness  
 426 and perihelion,  $\text{LAG} = +16 \pm 2$  days, that may be a thermal lag or due to the pole pointing  
 427 toward the sun at that time, or a combination of both (Figure 5).

428

429 The absolute magnitude  $\langle m(1,1) \rangle = 8.1 \pm 0.1$ . The maximum magnitude at the LAG  
 430 value is  $m(1, \text{LAG}) = 7.7 \pm 0.1$ .

431

432 *Turn on, turn off distances, and break point.* Figures 4 and 5 allow the determination of  
 433 the turn on distance. We find  $R_{ON} = -4.2 \pm 0.1$  AU,  $R_{OFF} = -6.0 \pm 0.2$  AU and  $T_{ON} = -400 \pm 40$   
 434 d and  $T_{OFF} = -830 \pm 15$  d. Thus  $R_{SUM} = 10.5 \pm 0.2$  AU and  $T_{ACTIVE} = 1904 \pm 43$  d.

435  
 436 For comparison comets 1P/Halley and 9P/Tempel 1 turned on at  $R_{ON} = -6.15$  and  
 437  $-3.5$  AU respectively, while their  $R_{SUM}$  was  $R_{SUM} = 18.7$  AU and  $7.7$  AU. Their active time  
 438 was  $T_{ACTIVE} = 1992$  d and  $1070$  d. We see that 103P is intermediate between the two.

439  
 440 This comet also belongs to the class of comets that exhibit a break point in their  
 441 SLC. Other members of this class are C/1995 O1 Hale-Bopp, 1P/Halley, 81P/Wild 2,  
 442 21P/Giacobini-Zinner, and 9P/Tempel 1 (Papers I-VI). Two linear laws are needed to  
 443 describe the behavior of this comet after turn on, and they change slope at a break point  
 444 located at  $R_{BP} = -1.20 \pm 0.1$  AU before perihelion, and magnitude  $m_{BP} = 9.4 \pm 0.1$ . The slope  
 445 of the first linear law is  $n = +9.44 \pm 0.05$  while the second linear law has  $n = +5.70 \pm 0.04$ .  
 446 The first value can be compared with the corresponding values of comets Hale-Bopp,  
 447 1P/Halley and 9P/Tempel 1,  $+10.3$ ,  $+8.9$  and  $+7.7$  respectively.

448  
 449 In paper VI it is shown that the preferred explanation for the break point, is the  
 450 change from sublimating something more volatile than  $H_2O$ , to sublimating  $H_2O$ .

451  
 452 *Composition.* Delsemme (1983) has a plot of production rate of several molecules,  $H_2O$ ,  
 453  $CO_2$  and  $CO$  vs heliocentric distance. The water ice curve shows curvature at 2 AU but  
 454  $CO$  or  $CO_2$  are in a linear regime. Since the SLC after turn on does not exhibit curvature  
 455 in any of the above comets (1P, 9P, HB, 103P), it is safe to conclude that sublimation is  
 456 not controlled by water ice (up to the break point). For comet 103P the controlling  
 457 substance at turn on may be  $CO$  or  $CO_2$  ice.  $CO_2$  has been detected spectroscopically  
 458 (Weaver et al. 1994) finding a  $CO_2/H_2O$  ratio  $\sim 4\%$ . The spectrum was observed by  
 459 ISOPHOT, SWS and ISOCAM, and  $H_2O$  and  $CO_2$  were detected, but not  $CO$  (Colangeli et  
 460 al., 1999; Crovisier et al., 1999, 2000). Thus it seems safe to conclude that the large  
 461 slope after turn on is due to  $CO_2$ .

462  
 463 Thus the shape of the SLC at turn on gives some idea of the substance that  
 464 controls sublimation.

465

466 *Photometric-age and time-age* From Figure 4 we measure an amplitude of the  
 467 secular light curve  $A_{\text{SEC}}(1,1) = 10.8 \pm 0.1$  in 1997. For comparison comets 1P/Halley and  
 468 9P/Tempel 1 had  $A_{\text{SEC}} = 10.8$  and 9.0. From a sample of 27 comets (Paper VI), it is  
 469 apparent that there is a maximum observed value of  $A_{\text{SEC}} = 11.55 \pm 0.1$  mag. 103P is  
 470 close to that maximum value, implying that we are seeing a relatively young object.

471

472 Then using  $R_{\text{SUM}} = 10.5$  AU and Equation (1) we find a photometric-age P-AGE  
 473  $(1,1) = 13 \pm 2$  cy, a relatively young object. From Figure 5 and Equation (2), we find T-  
 474 AGE =  $5 \pm 1$  cy.

475

476 In Paper VI comets have been classified by size and age. Smaller than 1.5 km in  
 477 diameter are dwarf, while those with  $3 \text{ cy} < \text{P-AGE}(1,1) < 30 \text{ cy}$ , are young. *According to*  
 478 *this classification 103P is a young dwarf comet.*

479

480 *Activity post-aphelion* Above we found the turn off point located at  $R_{\text{OFF}} = -5.4 \pm 0.1$  AU.  
 481 Since the aphelion distance of this comet is  $Q = 5.86$  AU the turn off point is after aphelion.  
 482 Figures 4 and 5 show that there is activity *after* aphelion. Thus this comet belongs to the  
 483 group of *spill-over comets*, those whose activity spills over from one orbit to the next.  
 484 Alternatively spill-over comets can be defined as *“those whose magnitude do not reach to*  
 485 *nuclear when the solar distance reaches to aphelion”*.

486

487 Other probable members of this group (see Paper I) are 81P/Wild 2, 19P/Borrelly  
 488 and 21P/Giacobinni-Zinner. Comparing their photometric age, P-AGE (13 cy, 14 cy, 20  
 489 cy, respectively), it is apparent that all spill-over comets are young objects. The  
 490 photometric-age of 103P was found above to be  $13 \pm 2$  cy, in agreement with this  
 491 conclusion. This comet should be observed after aphelion, to pinpoint the precise  
 492 location of the turn off, but this requires reaching to magnitude 26 and thus a large mirror.

493

494 After aphelion the comet is in a peculiar situation. Its brightness is decreasing in  
 495 spite of the fact that it is approaching the sun.

496

497 *1991 and 2004 apparitions* To complete the study of this comet, we have compiled the  
 498 1991 and the 2004 secular light curves, defined with fewer observations.

499

500 In 1991 the envelope of the comet was identical to that of 1997, thus the  
 501 physical parameters deduced are very similar to those of 1997 and are listed in Figure 6.

502

503 In 2004 there are only 25 observations (Figure 7). However in this apparition the  
 504 comet perihelion jumped from 0.953 AU in 1991 to 1.036 AU in 2004. There was then a  
 505 jump of 0.0833 AU. The comet received less solar energy, and this is reflected in the  
 506 absolute magnitude  $m(1,LAG)$  that jumped from 7.4 in 1991 to 8.9 in 2004, a jump of 1.5  
 507 magnitudes. This is the *perihelion effect* described in Paper VI and defined as: “a change  
 508 in the absolute magnitude due to a jump in perihelion distance”. The parameters of this  
 509 apparition are listed in Figure 7.

510

511 *Future observational conditions* This comet will have a close encounter with Earth on  
 512 October 21<sup>st</sup>, 2010, at  $\Delta = 0.12$  AU. The object is in the observing list of the Arecibo radio  
 513 telescope (Harmon et al., 1999). The encounter with the EPOXI spacecraft is scheduled  
 514 to take place on November 4<sup>th</sup>, 2010, 24 days before perihelion.

515

#### 516 4. Water Budget

517

518 We define the water budget, WB, as the total amount of water expended by the  
 519 comet in a single orbit. Festou (1986) found a correlation between the water production  
 520 rate  $Q_{H_2O}$  and the reduced visual magnitude for many comets of the form

521

$$522 \quad \text{Log } Q_{H_2O} = a - b m(1,1) \quad (4)$$

523

524 Subsequently many other researchers have found the same correlation (Roettger et  
 525 al., 1990; Jorda et al., 2008; de Almeida et al., 1997). In the latest determination by Jorda  
 526 et al. (2008) the following values for the parameters a and b were found  $a = 30.675$ ,  $b =$   
 527  $-0.2453$  (5)

528

529 Using this empirical correlation it is possible to convert the reduced magnitudes  
 530 presented in the time plot (Figure 5) to water production rate, day by day. The sum of  
 531 these values from  $T_{ON}$  to  $T_{OFF}$  gives the water budget in kg

532

533  $T_{OFF}$

$$WB = \sum_{T_{ON}} Q_{H_2O}(t) \Delta t \quad (6)$$

In Figure 8 we plot the daily water production rate vs time to show how it increases as a function of time. We also plot the same value for comet 9P/Tempel 1 for comparison, since this comet was visited by a spacecraft and has been well studied (A'Hearn et al. 2005, and papers therein). We conclude that 103P produces about 1.47 times more water than comet 9P in spite of being much smaller in diameter (1.43 vs 5.5 km).

Let us define a new age, the water budget age, thus

$$WB\text{-AGE [cy]} = 3.58 \cdot 10^{+11} / WB$$

The constant is chosen so that comet 28P/Neujmin 1 has a WB-AGE of 100 cy. The WB-AGE is calculated for several comets in Table 2. We find that the WB-AGE = 19 cy for 103P. Compare this value with a WB-AGE = 28 cy for comet 9P/Tempel 1 once again indicating that 103P is younger (more active) than 9P.

In Table 2 we compare the water production rates of several comets to place 103P in perspective. We list the amplitude of the secular light curve,  $A_{SEC}$ , the photometric age P-AGE(1,1), the photometric age P-AGE(1,q), and the new water budget age, WB-AGE. Notice that WB spans a range of 5 orders of magnitude while P-AGE spans a range of three orders of magnitude. Column 8 of Table 2 gives the WB scaled to 1P/Halley.

All the parameters of 103P have intermediate values, and thus we have to conclude that we are dealing with a relatively young object. Notice for example that its P-AGE(1,1) = 13 cy compares well with its WB-AGE = 19 cy. These values for comet 9P/Tempel 1 were P-AGE = 21 cy and WB-AGE = 28 cy. The WB scaled to comet 1P/Halley is also of great interest. We find that comet 103P expended 3.4 % of the water of 1P, while 9P expended 2.3 %.

## 5. Validation of the concept of Photometric Age



567

568 In Figure 9 the envelopes of several comets are compared taken from Paper VI.  
569 We see that older comets are nested inside younger objects. In other words, P-AGE  
570 classifies comets by shape of the SLC. Additionally Figure 9 shows that as a function  
571 of age,  $A_{SEC}$  and  $R_{SUM}$ , diminish in value. That is, a comet has to get nearer to the sun  
572 to get activated, and it is less and less active as it ages.

573

574 From Figure 9 and Table 2 the conclusion is that WB and P-AGE measure  
575 activity of a comet and that activity diminishes monotonically as a function of age.

576

## 577 **6. Applicability of the concept of $Af\rho$**

578

579 The concept of  $Af\rho$  was developed by A'Hearn et al. (1984) to quantify the dust in  
580 a comet, using a radial model of constant velocity of expansion. In this way  
581 measurements carried out with different apertures, at different times and of different  
582 comets, are directly comparable. However, there are restrictions to the applicability of  
583 this concept. 1) The model is not applicable within a few 100 km of the nucleus  
584 because the dust is still being accelerated by the gas. 2) Beyond about  $10^5$  km the  
585 model also fails because solar radiation pressure affects the motion of the dust. 3) If  
586 the comet has already turned off in its activity but a cloud of old dust moves with it, the  
587 model is not right either. 4) Any comet with short term variability also fails to comply  
588 with the  $Af\rho$  concept. 5) Additionally, the model was not developed to deal with comet  
589 tails or trails. 6) Since what is being measured is the dust, observations have to be  
590 made in the red or infrared part of the spectrum. Visual data, like the observations  
591 presented in the secular light curves, measures mostly the gas represented by the  $C_2$   
592 molecular bands.

593

594 In general it is found that the  $Af\rho$  model works best for a symmetric coma in  
595 steady state, from  $10^2$  to  $10^5$  km approximately. In this range it is expected that the  
596 value will be constant with aperture. If the dust (and thus the magnitude) follows a  $1 / \rho$   
597 distribution, then  $Af\rho$  will be constant at every aperture size. However notice that a  $1 / \rho$   
598 distribution gives an infinite integral for the total magnitude. Thus *necessarily* the  
599 intensity must decrease faster than  $1 / \rho$  at large distances or the magnitude will not  
600 converge.

601

602 Since the units of  $Af\rho$  are cm, the question is what is the physical meaning of this  
 603 quantity. In that regard it is useful to point out that Arpigny et al. (1986) have found a  
 604 correlation between  $Af\rho$  and dust production in tons (A'Hearn, 2009, personal  
 605 communication). They find that a value of  $Af\rho$  of 1000 cm corresponds to a mass loss  
 606 rate of dust of roughly 1000 kg per second. Alternatively an  $Af\rho$  of 1 cm would  
 607 correspond to a mass loss rate of 1 kg per second. This result ignores the size  
 608 distribution of particles among other parameters, but is a useful way to interpret the  
 609 meaning of  $Af\rho$ . Unfortunately, the correlation has never been published.

610

611 The formula developed by A'Hearn et al. (1984) and also used by Meech et al.  
 612 (2009) is

613

$$614 \quad A(\theta)f\rho = [2.467 \cdot 10^{19} R^2 \Delta 10^{0.4(m_{\odot} - m)}] / \rho \quad (7)$$

615

616 where  $\theta$  = phase angle in degrees,  $R$  = Sun-comet distance in AU,  $\Delta$  = Earth-comet  
 617 distance in AU,  $m_{\odot}$  = solar magnitude in the red = -27.1,  $m$  = observed magnitude,  $\rho$  =  
 618 radius of aperture in arc seconds. This equation implies that  $Af\rho$  is a function of the  
 619 Sun-comet-Earth angle. Schleicher et al. (1998) derived a quadratic fit to the comet  
 620 Halley data of the form

621

622

$$623 \quad \Delta \text{Log } A(\theta)f\rho = -0.01807 \theta + 0.000177 \theta^2 \quad (8)$$

624

625 that they use to model comet 9P/Tempel 1 data. They mention that this phase function  
 626 works well for phase angles smaller than 45-50°. The value in Equation (8) may be  
 627 multiplied by -2.5 to convert to magnitudes.

628

629 That the application of the  $Af\rho$  concept is not straight forward can be plainly seen  
 630 comparing the results of Schleicher (2007) with those of Milani et al. (2007) for comet  
 631 9P/Tempel 1. Figure 4c of Schleicher (2007) shows an  $Af\rho$  peaking -25 days before  
 632 perihelion which is not in accord with the visual secular light curve of Ferrín (Paper III)  
 633 (Ferrin's Figure 2, which measures mainly the gas) peaking  $-10 \pm 5$  days before

634 perihelion. On the other hand Figure 4 of Milani et al. (2007) shows  $Af\rho$  peaking -  
635 85 days before perihelion. None of the results agree with the fact that the gas and dust  
636 must be coupled on physical grounds. These results would be very difficult to reconcile  
637 with physical theories and would require fancy explanations.

638  
639 In view of the limitations of the applicability of the  $Af\rho$  concept, it is always wise to  
640 check if the hypothesis of its constancy vs aperture is fulfilled. Going back to our  
641 measurements, in Figure 10a we see the magnitude of the comet in increasing  
642 apertures, used to derive the infinite aperture magnitude (IAM) the night 050112. It can  
643 be seen that the IAM is reached for apertures larger than  $42'' = 73.000$  km, much larger  
644 that apertures typically used in cometary photometry. That is why we emphasize the  
645 need to use this curve of growth method to derive the total magnitude of the comet. In  
646 Figure 10b, we plot the  $Af\rho$  value vs measuring aperture calculated with equation (7) to  
647 see if the hypothesis of constant  $Af\rho$  with  $\rho$  is fulfilled. We see that for the night of  
648 050112 it is not.

649  
650 An identical result is found for the night 060229. An aperture of at least  $10'' =$   
651  $31.000$  km is needed to extract all the flux. Once again we find that the conditions to  
652 have a constant value are not fulfilled. This is not surprising in view that the comet  
653 exhibits a tail and thus solar radiation pressure is important, distorting the even flow of  
654 the dust and making the conditions to have a constant  $Af\rho$  invalid.

655  
656 Schleicher (2007) finds a similar situation for comet 9P/Tempel 1. He finds (his  
657 Figure 3) that  $Af\rho$  is strongly dependent on  $\rho$  for five dates. The question then arises, if  
658  $Af\rho$  is a function of  $\rho$ , then what is the correct value of  $Af\rho$ ? Schleicher (2007) decides  
659 to normalize all values to  $10^4$  km from the nucleus and at a phase angle of  $41^\circ$ . These  
660 are arbitrary numbers that do not have attached any physical meaning. We prefer to  
661 correct to zero phase angle, and to identify the correct  $Af\rho$  value as the one that  
662 corresponds to the IAM derived in Figure 10a, and thus to the minimum value of  $Af\rho$   
663 corresponding to those apertures. In this case the correct value of  $Af\rho$  is smaller than  
664 what we would derive using other criteria.

665

666 Our phase angles are given in Table 1. We find that  $A(\theta)f\rho$  had a value of  
 667 around 55 cm on 050112 and correcting to  $\theta = 0^\circ$  with Equation (8), we find 106 cm.  
 668 For the date 060229 we find a  $A(\theta)f\rho = 27$  cm, and when corrected to  $\theta = 0^\circ$  we find  
 669  $A(0)f\rho = 37$  cm. These correspond to mass loss rates of 106 kg/s and 37 kg/s  
 670 respectively. The value decreases with distance to the Sun as expected theoretically.

671  
 672 In conclusion, in spite of the fact that the concept of  $Af\rho$  is a useful one,  
 673 researchers have not always been aware of its limitations. The value of  $Af\rho$  must be  
 674 checked as a function of aperture to verify the applicability of the concept. Thus  
 675 previous determinations of  $Af\rho$  should probably be revised downward.

676

## 677 7. Mass loss and remaining time

678

679 From Table 2 it is possible to deduce that the comet lost  $1.88 \times 10^{10}$  kg of water in  
 680 the 1997 apparition. However we are interested in the total mass loss. To calculate it  
 681 we need the dust to gas mass ratio,  $\delta$ . The values of  $Af\rho$  deduced in a previous  
 682 section are of no help because they are far from perihelion and are non-constraining.  
 683 Sykes and Walker (1992) favor a mean value  $\delta = 2.9$  for a sample of several comets  
 684 while Singh et al. (1992) give values from 0.5 to 3. With this information it is possible to  
 685 calculate the thickness of the layer lost per apparition using the formula

686

$$687 \Delta r = (\delta + 1) WB / 4 \pi r^2 \rho \quad (9)$$

688

689 where  $r$  is the radius and  $\rho$  the density. This equation comes from the fact that the  
 690 density is given by  $\rho = \Delta M / \Delta V$ .  $\Delta V$ , the volume removed, is given by  $\Delta V = 4\pi r^2 \Delta r$ . And  
 691  $\Delta M$ , the mass removed, is given by  $\Delta M_{H_2O} + \Delta M_{DUST} = WB (1 + \Delta M_{DUST}/WB)$ . For the  
 692 density we are going to take a value of  $530 \text{ kg/m}^3$  which is the mean of many  
 693 determinations compiled in Paper I. The resulting values of  $\Delta r$  are compiled in Table 2  
 694 for 14 comets.

695

696 From Table 2 we see that comet 103P lost 34 m in radius in the 1997 apparition.  
 697 Since the radius of this comet is only 570 m, the ratio  $r_N / \Delta r = 17$ . This calculation implies  
 698 that the comet will sublimate away in only 17 additional revolutions, if the mass loss rate  
 699 is constant. This is the remaining time left for this comet, and it is a very small time ( $\sim 109$

700 y). However this is dependent on the dust to gas mass ratio assumed. Future  
701 observations should be acquired to follow the rapid sublimation of this comet and to  
702 pinpoint more precisely its remaining time.

703

## 704 **8. Comets Visited by Spacecraft**

705

706 From Table 2 and Figure 11 we find that by chance all comets that have been  
707 visited by spacecraft are young: 1P/Halley (7 cy), 9P/Tempel 1 (21 cy), 19P/Borrelly (14  
708 cy), 81P/Wild 2 (13 cy). 103P/Hartley 2 follows the same trend with  $P=AGE = 13$  cy.  
709 Thus we expect the surface of 103P to resemble that of previous comets.  
710 67P/Churyumov-Gerasimenko will be visited in 2014 by Rosetta. This comet has  $P-$   
711  $AGE = 32$  cy (Paper I) and thus it should present a slightly older surface.

712

713 What would be interesting to see is the surface of a really old object, a methuselah  
714 comet ( $P-AGE > 100$  cy). Several are available. The following photometric ages have  
715 been extracted from the *Atlas of Secular Light Curves* (Paper VI) and unpublished results:  
716 107P/Wilson-Harrington (760 cy), 133P/Elst-Pizarro (280 cy), 169P/NEAT = 2002 EX12  
717 (245 cy), P/2006 T1 Levy (100 cy), 162P/Siding-Spring (230 cy). Not so old comets but  
718 still methuselah are 2P/Encke (102 cy) and 28P/Neujmin 1 (100 cy). A spacecraft  
719 mission to any methuselah object would be of great scientific interest. It is specifically  
720 predicted that a Methuselah comet will have a more extreme surface morphology, than the  
721 cometary surfaces that have been imaged up to now.

722

## 723 **9. Conclusions and results**

724 The main conclusions of this work are:

725

726 a) We have shown that for comets that exhibit a coma, the best estimate of the brightness  
727 is the infinite aperture magnitude, IAM, obtained using a curve of growth method (Figure  
728 2). This is usually 0.4 - 2.0 magnitudes brighter than magnitudes deduced with smaller  
729 apertures (Figures 1, 2, Section 2).

730

731 b) Of the order of 30 photometric parameters are measured and listed in the plots of this  
732 comet, over 20 of them new (Figures 4 to 7). The turn on point of activity is  $-4.2 \pm 0.1$  AU  
733 from the Sun, which corresponds to  $-400 \pm 40$  d before perihelion. The total active time is

734  $T_{\text{ACTIVE}} = 1904 \pm 43$  d. For comparison the active time of comets 1P/Halley and  
 735 9P/Tempel 1 are  $T_{\text{ACTIVE}} = 1992$  and  $1069$  days. The comet exhibits a lag between the  
 736 maximum brightness and perihelion,  $\text{LAG} = +16 \pm 2$  days that may be due to a thermal lag  
 737 or to the pole pointing to the sun at that time, or a combination of both (Figures 4 and 5).

738

739 c) In Paper VI comets are classified according to their age and diameter. It is proposed  
 740 there that comets with  $4 < \text{P-AGE} < 30$  cy are young, while comets with  $D < 1.5$  km are  
 741 dwarf objects. In Section 3 we find the photometric age  $\text{P-AGE} = 13 \pm 2$  cy, while the  
 742 diameter found from the literature is  $1.14 \pm 0.16$  km. Thus according to the above  
 743 classification 103P is a *young dwarf comet*. For comparison comets 1P/Halley and  
 744 9P/Tempel 1 have photometric ages  $\text{P-AGE} = 7.1$  cy and  $\text{P-AGE} = 22$  cy (Paper VI) and  
 745 diameters  $9.8$  km and  $5.5$  km.

746

747 d) The nucleus is *very active* as can be deduced from the fact that the amplitude of the  
 748 SLC is  $A_{\text{SEC}} = 10.8 \pm 0.1$  mag in 1997. For comparison comets 1P and 9P have  $A_{\text{SEC}} =$   
 749  $10.8$  and  $9.0$  mag. From a sample of 27 comets (Paper VI), it is apparent that there is a  
 750 maximum value of  $A_{\text{SEC}} = 11.55 \pm 0.1$  mag. 103P is close to that maximum value, implying  
 751 that we are seeing a relatively young object (Figures 4 and 5).

752

753 e) The validity of the concept of photometric age, P-AGE, is studied comparing the  
 754 envelopes of several comets. It is apparent that older comets are nested inside the  
 755 envelope of younger comets. The conclusion is that P-AGE classifies comets by shape of  
 756 their secular light curve (Figure 9). This plot also shows that as a function of age, the  
 757 amplitude of the secular light curve,  $A_{\text{SEC}}$ , and  $R_{\text{SUM}} = -R_{\text{ON}} + R_{\text{OFF}}$ , decrease in value. The  
 758 comet has to get nearer to the sun to get activated and its activity is less and less (Section  
 759 5).

760

761 f) This comet belongs to the class of *spill-over* comets defined in Paper VI. After  
 762 remaining active up to aphelion, the comet spills-over its activity into the next orbit. The  
 763 other comets that populate this class are also young (Figure 4 and 5).

764

765 g) 103P also belongs to the family of *comets that exhibit a break point* in their SLC. Two  
 766 linear laws change slope at a break point located at  $R_{\text{BP}} = -1.20 \pm 0.1$  AU before perihelion,  
 767 and magnitude  $m_{\text{BP}} = 9.4 \pm 0.1$ . The slope of the first linear law after turn on is  $n = +9.44$ .

768 This value can be compared with the slopes of comets Hale-Bopp, 1P/Halley and  
769 9P/Tempel 1: +10.3, +8.92 and +7.7 respectively. Since the SLC after turn on does not  
770 exhibit curvature in any of these comets, it is safe to conclude that sublimation is not  
771 controlled by water ice. The controlling substance may be CO or CO<sub>2</sub> ice. CO<sub>2</sub> has been  
772 detected spectroscopically.

773

774 h) The water budget of this comet is calculated. The comet expends  $1.88 \cdot 10^{10}$  kg of water  
775 per apparition vs  $1.28 \cdot 10^{10}$  kg for comet 9P/Tempel 1. A new water-budget age is defined  
776 and it is found that WB-AGE = 19 cy vs WB-AGE = 28 cy for 9P. These results imply that  
777 this is a comet younger than 9P/Tempel 1.

778

779 i) The values of  $A_{fp}$  are calculated on two dates and we find dust production rates of 106  
780 and 37 kg/s, decreasing with solar distance as expected. The applicability of the concept  
781 of  $A_{fp}$  is studied using a double plot of magnitude and  $A_{fp}$  vs aperture. In this way infinite  
782 aperture magnitudes and infinite aperture  $A_{fp}$ s are deduced (Figure 10 and Section 6).

783

784 j) The thickness of the layer lost per apparition is calculated, and we find  $\Delta r = 34$  m where  
785  $r$  is the radius. Since the radius of this comet is  $r = 570$  m, it is found that at the present  
786 rate the comet may disappear in only 17 revolutions or  $\sim 109$  y. However this is  
787 dependent on the dust to gas mass ratio assumed which is uncertain.

788

789 k) By chance all comets visited by spacecraft have small photometric ages and thus are  
790 young objects (Figure 11 and Section 8). 103P follows the same trend. Thus it is  
791 expected that the surface morphology that will be found in future EPOXI images should be  
792 very similar to that of previous comets. It is suggested that any new mission to a comet  
793 should be made to a really old object and several are proposed (107P, 133P, 162P, 169P,  
794 and P/2006 T1).

795

796 The “*Atlas of Secular Light Curves of Comets*” in color as well as numerous tables  
797 of cometary physical properties are available and can be downloaded from the web site:

798 <http://webdelprofesor.ula.ve/ciencias/ferrin>.

799

800

801

**802 10. Acknowledgements**

803 To two unknown referees for having contributed significantly to the scientific  
804 improvement of this paper. To the Council for Scientific, Technologic and Humanistic  
805 Development of the University of the Andes for their support through grant number C-  
806 1281-04-05-B. To the Centro de Investigaciones de Astronomía, CIDA, for the time  
807 granted to observe comets. The help of the night assistants and professional observers,  
808 Ubaldo Sanchez, Freddy Moreno, Orlando Contreras, Gregory Rojas, Daniel Cardozo,  
809 Faviola Moreno, Cecilia Mateu, and Carlos Castillo, is highly appreciated. We thank the  
810 members of the comet-obs web site for providing the partial aperture magnitudes: I.  
811 Almendros, F. Baldris, J. Barceló, M. Camarasa, M. Campas, M. Casao, E. Cortés, J.  
812 Castellanos, CEAMIG-REA, J. A. de los Reyes, J. L. Dorestes, F. Fratev, F. García, T. C.  
813 García, J. García M., J. Lacruz, L. and S. Lahuerta, D. Mendicini, F. Montalbán, R.  
814 Morales, R. Naves, S. Pastor, E. Reina, M. Reszelsky, D. Rodríguez, J. L. Salto, J.  
815 Sanchez, J. R. Vidal.  
816  
817



818 **11. References**

- 819 A'Hearn, M., Schleicher, D. G., Millis, R.L., Feldman, P.D., Thompson, D.T., 1984.  
820 Comet Bowell 1980b. *AJ*, 89, 579-591.
- 821 A'Hearn, M.F. and 32 colleagues, 2005. Deep Impact: Escavating Comet Tempel 1.  
822 *Science*, 310, 258-264
- 823 A`Hearn, M.F., Combi, M.R., 2007. Deep Impact at Comet Tempel 1. *Icarus*, 187, 1-3.
- 824 Arpigny, C., Dossin, F., Woszczyk, A., Donn, B., Rahe, J., Wyckoff, S., 1986.  
825 Presentation of an Atlas of cometary spectra. In *Asteroids, comets, meteors II*;  
826 *Proceedings of the International Meeting, Uppsala, Sweden, June 3-6, 1985*  
827 (A87-11901 02-90). Uppsala, Sweden, Astronomiska Observatoriet.
- 828 Chen, J., Jewitt, D., 1994. On the Rate at Which Comets Split. *Icarus*, 108, 265-271.
- 829 Colangeli, L., Epifani, E., Brucato, J.R., Bussoletti, E., de Sanctis, C., Fulle, M., Mennella,  
830 V., Palomba, E., Palumbo, P., Rotundi, A. 1999. Infrared spectral observations of  
831 comet 103P/Hartley 2 by ISOPHOT. *A&A*, 343, L87-L90.
- 832 Crovisier, J., Encrenaz, Th., Lellouch, E., Bockelee-Morvan, D., Altieri, B., Leech, K.,  
833 Salama, A., Griffin, M.J., de Graauw, Th., van Dishoeck, E.F., Knacke, R., Brooke,  
834 T.Y. 1999. ISO Observations of short period comets. In "The Universe seen by  
835 ISO". P. Cox and M.F. Kessler (Eds.), ESA SP427, 137-140.
- 836 Crovisier, J., Brooke, T.Y., Leech, K., Bockelee-Morvan, D., Lellouch, E., Hanner, M.S.,  
837 Altieri, B., Keller, H.U., Lim, T., Encrenaz, Salama, Griffien, M., de Graauw, T., van  
838 Dishoeck, E., Knacke, R.F. 2000. The thermal infrared spectra of comets  
839 Hale-Bopp and 103P/Hartley 2 oberved with the infrared Space Observatory.  
840 In *Thermal Emission Spectroscopy and Analysis of Dust, Disks, and*  
841 *Regoliths*. M.L. Sitko, Al.L. Sprague and D.K. Lynch (Eds.). ASP Conference  
842 Series, 196, 109-117.
- 843 De Almeida, A.A., Singh, D.D., Hubner, W.F., 1997. Water release rates, active areas,  
844 and minimum nuclear radius derived from visual magnitudes of comets-an  
845 application to comet 46P/Wirtanen. *PSS*, 45, 681-692.
- 846 Delsemme, A.H., 1983. Chemical Composition of Cometary Nuclei. P. 92, in *Comets*,  
847 L.L. Wilkening, Editor. Univ. Of Arizona Press, Tucson, AZ.
- 848 Ferrín, I., 2005a. Secular Light Curve of Comet 28P/Neujmin 1, and of Comets Targets  
849 of Spacecraft, 1P/Halley, 9P/Tempel 1, 19P/Borrelly, 21P/Grigg-Skejellerup,  
850 26P/Giacobinni-Zinner, 67P/Chryumov-Gersimenko, 81P/Wild 2. *Icarus*  
851 178, 493-516. Paper I.
- 852 Ferrín, I., 2005b. Variable Aperture Correction Method in Cometary Photometry,  
853 *ICQ* 27, p. 249-255. Paper II.
- 854 Ferrín, I., 2006. Secular Light Curve of Comets, II: 133P/Elst-Pizarro, an asteroidal  
855 belt comet. *Icarus*, 185, 523-543. Paper III.
- 856 Ferrín, I., 2007. Secular Light Curve of Comet 9P/Tempel 1. *Icarus*, 187, 326-331.  
857 Paper IV.
- 858 Ferrín, I., 2008. Secular Light Curve of Comets 2P/Encke, a comet active  
859 at aphelion. *Icarus*, 197, 169-182. Paper V.
- 860 Ferrín, I., 2010. Atlas of Secular Light Curves of Comets. *PSS*, 58, 365-391.  
861 is available in color at <http://webdelprofesor.ula.ve/ciencias/ferrin>. Paper VI.
- 862 Festou, M.C., 1986. The derivation of OH gas production rates from visual magnitudes  
863 Of comets. In *Asteroids, Comets, Meteors II*, C.I. Lagerkvist et al., Editors,  
864 299-303. Uppsala Univ. Press, Uppsala, Sweden.
- 865 Fink, U., Hicks, M.P., Fevig, R.A., 1999. Production rates for the Stardust Mission Target:  
866 81P Wild 2. *Icarus*, 141, 331-340.
- 867 Green, D.W.E., 1997. *ICQ Guide to observing comets*. Cambridge, MA; Smithsonian  
868 Astrophysical Observatory, p. 100-103.

- 869 Green, D.W., 2006. International Comet Quarterly, 28, 81.
- 870 Groussin, O., Lamy, P., Jorda, L., Toth, I., 2004. The Nuclei of Comets 126P/IRAS  
871 and 103P/Hartley 2. A&A, 419, p. 375-383.
- 872 Harmon, J. K., Campbell, D. B., Ostro, S.J., Nolan, M.C., 1999. Radar observations  
873 of comets, Planetary and Space Science, 47, p. 1409-1422.
- 874 Jorda, L., Crovisier, J., Green, D.W.E., 2008. The correlation between water production  
875 rates and visual magnitudes of comets. In Asteroids, Comets, Meteors 1991,  
876 285-288. Lunar and Planetary Institute, LPI Contribution No. 1405, paper id  
877 8046, Houston, TX, USA.
- 878 Jorda, L., Lamy, P., Groussin, O., Toth, I., A'Hearn, M. F., Peschke, S., 2000. ISOCAM  
879 Observations of cometary nuclei. In Proceedings of ISO Beyond Point Sources,  
880 Studies of Extended Infrared Emission, (R. J. Lureijs et al., Editors), p. 61,  
881 ESA SP-455, Noordwijk, The Neatherlands.
- 882 Licandro, J., Tancredi, G., Lindgren, M., Rickman, H., Hutton, R. G., 2000. CCD  
883 Photometry of Cometary Nuclei, I: Observations from 1990-1995. Icarus,  
884 147, p. 161-179.
- 885 Lisse, C.M., Fernandez, Y.R., Reach, W.T., Bauer, J.M., A'Hearn, M.F., Farnham, T.L.,  
886 Groussin, O., Belton, M.J., Meech, K.J., Snodgrass, C.D., 2009. PASP, 121,  
887 968-975.
- 888 Lowry, S.C., Fitzsimmons, A., 2001. CCD Photometry of Distant Comets, II. A&A,  
889 365, p. 204-213.
- 890 Lowry, S.C., Fitzsimmons, A., Collander-Brown, S., 2003. CCD Photometry of Distant  
891 Comets, III. A&A, 397, p. 329-343.
- 892 Milani, G.A., Szabo, Gy.M., Sostero, G., Trabatti, R., Ligustri, R., Nicolini, M., Facchini,  
893 M., Tirelli, D., Carosati, D., Vinante, C., Higgins, D., 2007. Photometry of Comet  
894 9P/Tempel 1 during the 2004/2005 approach and the Deep Impact module  
895 impact. Icarus, 187, 276-284.
- 896 Meech, K.J., Pittichova, J., Bar-Nun, A., Notesco, G., Laufer, D., Hainaut, O.R., Lowry,  
897 S.C., Yeomans, D.K., Pitts, M. 2009. Activity of comets at large heliocentric  
898 distances pre-perihelion. Icarus 201, 719-739.
- 899 Roettger, E.E., Feldman, P.D., A'Hearn, M.F., Festou, M.C., 1990. Comparison of water  
900 production rates from UV spectroscopy and visual magnitudes for some recent  
901 comets. Icarus, 86, 100-114.
- 902 Schleicher, D., G., Millis, R.L., Birch, P.V., 1998. Narrowband Photometry of Comet  
903 P/Halley: Variation with Heliocentric Distance, Season, and Solar Phase Angle.  
904 Icarus, 132, 397-417.
- 905 Schleicher, D., G., 2007. Deep Impact's target Comet 9P/Tempel 1 at multiple  
906 apparitions: Seasonal and secular variations in gas and dust production. Icarus,  
907 190, 406-422.
- 908 Singh, P.D., de Almeida, A.A., Huebner, W.F., 1992. Dust release rates and dust to  
909 Gas mass ratios of eight comets. An.J., 104, 848-858.
- 910 Sosa, A., Fernandez, J.A., 2009. Cometary masses derived from non-gravitational  
911 forces. MNRAS, 393, 192-214.
- 912 Snodgrass, C., Lowry, S.C., Fitzsimmons, A., 2006. Photometry of cometary nuclei:  
913 Rotation rates, colours and a comparison with Kuiper Belt Objects. MNRAS,  
914 385, 737-756.
- 915 Snodgrass, C., Meech, K.J., Hainaut, O.R., 2010. The nucleus of 103P/Hartley 2,  
916 target of The EPOXI mission. A&A, May 10, 2010, in press.
- 917 Sykes, M.V., Walker, R.G., 1992. The nature of comet nuclei. Asteroids, Comets,  
918 Meteors, 1991, 587-591.
- 919 Weaver, H.A., Feldman, P.D., McPhate, J.B., A'Hearn, M.F., Arpigny, C., Smith,

920  
921 T.E., 1994. Detection of CO Cameron band emission in comet P/Hartley 2 (1991  
922 XV) with the Hubble Space Telescope. Ap.J., 422, 374-380.  
923  
924  
925  
926  
927  
928  
929  
930  
931  
932  
933  
934  
935  
936  
937  
938  
939  
940  
941  
942  
943  
944  
945  
946  
947  
948  
949  
950  
951  
952  
953  
954  
955  
956  
957  
958  
959  
960  
961  
962  
963  
964  
965  
966  
967  
968  
969  
970

971 **Figure captions**

972 Figure 1. Comet 103P/Hartley 2 imaged with the 1 m Schmidt telescope of the National  
 973 Observatory of Venezuela, at f/3, on 2005, January 12<sup>th</sup>. Since large photometric  
 974 apertures have to be used to extract the whole flux, the image has previously been  
 975 cleaned of nearby stars using a cloning tool. The area between the two circles measures  
 976 the sky background. Both images have the same scale. Left: A normal stretching of the  
 977 image shows that an aperture of radius 20 pixels is apparently enough to extract a total  
 978 magnitude. Stretching refers to the maximum and minimum pixel intensity to display the  
 979 image in the computer monitor. The standard stretching is selected by the computer, who  
 980 does not know about preserving the flux. Thus the monitor displays a deceptively faint  
 981 image. Right: A forced stretching reveals a much larger coma than expected and a much  
 982 brighter comet. At least a 44 pixel radius is needed to extract a total magnitude (some  
 983 flux is still left out). This has been called the *insufficient CCD aperture error* (Paper II),  
 984 and manifests itself by producing measurements that lie much below the envelope of the  
 985 observations.

986  
 987 Figure 2. Derivation of an infinite aperture magnitude. It can be seen how the calibration  
 988 star and the comet increase in flux with increasing photometric apertures. The asymptotic  
 989 value is the infinite aperture magnitude, IAM. Notice the huge aperture needed to extract  
 990 the whole flux of the comet, much larger than apertures typically found in the literature.  
 991 Notice also how the calibration star #14 converges rapidly to its asymptotic value but still  
 992 needs an 8 pixel radius to retrieve an IAM.

993  
 994 Figure 3. Images of comet 103P/Hartley 2 taken with telescopes of the National  
 995 Observatory of Venezuela. Upper row, 1m Schmidt telescope working at f/3. Bottom  
 996 row, 1 m Reflector Telescope, at f/21. The information related to these images is  
 997 compiled in Table 1. North is at the top, East to the left. The two left images are  
 998 simultaneous observations. They are particularly interesting to compare because they  
 999 were taken with very different f/ ratios. The f/21 reflector looses about 0.4 mag. Even in  
 1000 the upper right hand image taken at R= 5.03 AU from the sun and magnitude  $R(\Delta,R)=$   
 1001 20.2, the comet displays a faint coma.  $V_{IAM}$  and  $R_{IAM}$  are infinite aperture magnitudes  
 1002 obtained by fitting an exponential decay function to magnitudes measured as a function of  
 1003 increasing CCD apertures (see text).

1004  
 1005 *Upper Left hand image:* 1m Schmidt, f/3. Date = 2005 01 12.19, Exposure = 21 min,  
 1006  $R_{IAM}(\Delta,R) = 17.1\pm 0.1$ ,  $\Delta t = +134$  d, R = 2.85 AU,  $\Delta = 2.40$  AU, RA = 07h 24m 05s, DEC =  
 1007  $+18^\circ 58' 28''$ , Filter = Clear. The image is 3.5'x5.0' in size.

1008  
 1009 *Upper Right hand image:* 1m Schmidt, f/3. Date = 2006 03 01.20, Exposure = 12 min,  
 1010  $R_{IAM}(\Delta,R) = 20.4\pm 0.2$ ,  $\Delta t = +135$  d, R = 5.03 AU,  $\Delta = 4.31$  AU, RA = 07h 24m 18s, DEC =  
 1011  $+18^\circ 55' 58''$ , Filter = Clear. The image is 3.5'x5.0' in size

1012  
 1013 *Lower Left hand image:* 1m Reflector, f/21. Date = 2005 01 12.17, Exposure = 45 min,  
 1014  $R_{IAM}(\Delta,R) = 17.0\pm 0.2$ ,  $\Delta t = +134$  d, R = 2.85 AU,  $\Delta = 2.40$  AU, RA = 07h 24m 05s, DEC =  
 1015  $+18^\circ 58' 28''$ , Filter = Clear. The image is 3.5'x5.0' in size.

1016  
 1017 *Lower Right hand image:* 1m Reflector, f/21. Date = 2005 01 14.23, Exposure = 50 min,  
 1018  $R_{IAM}(\Delta,R) = 17.8\pm 0.2$ ,  $\Delta t = +135$  d, R = 2.87 AU,  $\Delta = 2.39$  AU, RA = 07h 24m 18s, DEC =  
 1019  $+18^\circ 55' 58''$ , Filter = Clear. The image is 3.5'x5.0' in size

1020  
 1021

1022 Figure 4. Secular light curve of comet 103P/Hartley 2 in 1997, log plot. The slope  
 1023 5 line at the bottom of the plot in the form of a pyramid is due to the atmosphereless  
 1024 nucleus. The comet exhibits a well defined SLC, with a linear behavior before turn on  
 1025 indicating that it is controlled by a substance more volatile than water ice, probably CO<sub>2</sub> or  
 1026 CO. This is in agreement with the small photometric age, P-AGE= 13±2 comet years.  
 1027 The activity spills over into the next orbit as shown at right, where the brightness is ~5  
 1028 magnitudes above the nucleus. Notice the cluster of modern CCD observations. The  
 1029 error of the Snodgrass et al. observation (SMH) is contained inside the size of the symbol.  
 1030 TW= this work. LF= Lowry and Fitzsimmons (2001). CJ= Chen and Jewitt (1994).  
 1031 LTLRH= Licandro et al. LFCW= Lowry et al. (1999), SLF= Snodgrass et al. (2006),  
 1032 SMH= Snodgrass et al. (2010), GLJT= Groussin et al. (2004). L et al. = Lisse et al.  
 1033 (2009).

1034  
 1035 Figure 5. Secular light curve of comet 103/Hartley 2 in 1997, time plot. The comet  
 1036 exhibits a prominent belly as expected of a young object. There is a cluster of modern  
 1037 CCD observations on the right hand side. The error of the Snodgrass et al. observation  
 1038 (SMH) is contained inside the size of the symbol. Figure 5 is a text-book example of a  
 1039 “spill over comet” with a prominent belly.

1040  
 1041 Figure 6. Secular light curve of comet 103P/Hartley 2 in 1991, log plot. The comet  
 1042 exhibits a very small perihelion effect (q-effect), defined as a change in the perihelion  
 1043 magnitude  $m(1,LAG)$  as a result of a change in the perihelion distance,  $q$ . See text.

1044  
 1045 Figure 7. Secular light curve of comet 103P/Hartley 2 in 2004, log plot. From 1997 to  
 1046 2004 there was a change in  $m(1,1)$  of +1.5 magnitudes.

1047  
 1048 Figure 8. Water budget of 103P compared to the water budget of 9P/Tempel 1. Most of  
 1049 the sublimation takes place near perihelion, explaining the large slope at  $q$ . Although the  
 1050 comet is active at aphelion, the contribution to WB is negligible at that distance. The  
 1051 production rate of 103P is asymmetric with respect to perihelion with an asymmetry  
 1052 parameter of 1.76, in agreement with the asymmetry shown in Figure 5 in the time plot.

1053  
 1054 Figure 9. Validation of the concept of photometric age, P-AGE: envelopes of comets  
 1055 compared. It is apparent that older comets are nested inside the envelope of younger  
 1056 comets. The conclusion is that P-AGE classifies comets by shape of their secular light  
 1057 curve. On the left hand side, the comet number. On the right hand side, the photometric  
 1058 age. This plot also shows that as a function of age, the amplitude of the secular light  
 1059 curve,  $A_{SEC}$ , and  $R_{SUM} = -R_{ON} + R_{OFF}$ , decrease in value. The comet has to get nearer to the  
 1060 sun to get activated, and is less and less active.

1061  
 1062 Figure 10.  $A_{fp}$  of comet 103P. The  $A_{fp}$  is calculated as a function of aperture from  
 1063 Figure 2 and equation 7. Above the infinite aperture magnitude is calculated. Below it  
 1064 can be seen that  $A_{fp}$  does not stay constant with  $\rho$ , decreasing in value with larger  
 1065 apertures. The reason is that the coma was not spherically symmetric, and exhibited a  
 1066 tail. The  $A_{fp}$  model assumes a symmetric coma, not distorted by the solar wind pressure.  
 1067 What then is the correct value of  $A_{fp}$ ? We believe it is the value derived when the whole  
 1068 flux has been extracted, and this corresponds to the infinite aperture magnitude.

1069  
 1070 Figure 11. By chance, all comets visited by spacecraft are young. Comet 103P/Hartley 2,  
 1071 with a photometric age of 13 comet years, follows the same trend. Thus we do not have  
 1072 any idea of how an old cometary surface looks like. We would expect to find a surface

1073  
1074 morphology for 103P not very different from that of previously visited objects. A mission  
1075 to a really old comet would be scientifically very exciting. Cometary targets to old comets,  
1076 are suggested in the text (Section 9).  
1077  
1078  
1079  
1080  
1081  
1082  
1083  
1084  
1085  
1086  
1087  
1088  
1089  
1090  
1091  
1092  
1093  
1094  
1095  
1096  
1097  
1098  
1099  
1100  
1101  
1102  
1103  
1104  
1105  
1106  
1107  
1108  
1109  
1110  
1111  
1112  
1113  
1114  
1115  
1116  
1117  
1118  
1119  
1120  
1121  
1122  
1123

1124  
1125

Table 1. Observing Log of comet 103P/Hartley 2.

YYMMDD	$\Delta t$ [d]	Diameter=1m Type f/	$\Delta$ [AU]	R [AU]	$\alpha$ [ $^\circ$ ]	Expo [s]	$R_{IAM}(\Delta, R)$	$V_{IAM}(\Delta, R)$	$V_{IAM}(1, R)$
050112	+212	Schmidt f/3	2.40	2.85	19.7	1260	16.7 $\pm$ 0.1	17.2 $\pm$ 0.1	15.3 $\pm$ 0.1
050112	+212	Reflector f/21	2.40	2.85	19.7	2700	17.0 $\pm$ 0.1	17.5 $\pm$ 0.1	15.6 $\pm$ 0.1
050114	+214	Reflector f/21	2.39	2.87	19.4	3000	17.8 $\pm$ 0.1	18.3 $\pm$ 0.1	16.4 $\pm$ 0.1
060301	+625	Schmidt f/3	4.31	5.03	8.5	700	20.2 $\pm$ 0.2	20.7 $\pm$ 0.2	17.5 $\pm$ 0.2
070216	+1004	Schmidt f/3	4.92	5.49	9.7	834	>20.9 $\pm$ 0.3	>21.3	>17.6
070220	+1008	Schmidt f/3	4.92	5.78	9.6	1807	>21.3 $\pm$ 0.4	>21.7	>18.0

1126  
1127  
1128  
1129  
1130  
1131  
1132  
1133  
1134  
1135  
1136  
1137  
1138

YMD= Year, Month, Date.  $\Delta t$  [d] = time after perihelion.  $\Delta$  [AU] = Earth-comet distance. R [AU] = Sun-comet distance.  $\alpha$  [ $^\circ$ ] = phase angle. Expo [s] = Total Exposure Time.  $R_{IAM}(\Delta, R)$  = infinite aperture R-band magnitude at  $\Delta$ , R.  $V_{IAM}(\Delta, R)$  = equivalent V-band magnitude obtained using  $\langle V-R \rangle = 0.41 \pm 0.16$  for comet 103P (Paper II).  $V_{IAM}(1, R)$  = V-band magnitude reduced to  $\Delta = 1$  AU.

Table 2. Comparison of 103P/Hartley 2 with other comets, in order of increasing water budget age, WB-AGE. WB-AGE [cy] =  $3.58 \text{ E}+11 / \text{WB} [\text{kg}]$  and P-AGE [cy] =  $1440 / [A_{SEC} \cdot R_{SUM}]$ ;  $R_{SUM} = -R_{ON} + R_{OFF}$

Comet	WB [kg]	$R_{SUM}$ [AU]	$A_{SEC}$ (1,1)	P-AGE (1,1) [cy]	P-AGE (1,LAG) [cy]	WB-AGE (1,q) cy	WB -----% WB(1P)	$r_N$ [km]	$\Delta r_N$ [m]	$r_N$ ----- $\Delta r_N$
HB	7.66 E+12	52.1	11.5	2.3	2.3	0.047	1393	27	6.2	4388
1P	5.52 E+11	18.7	10.8	7.1	6.6	0.65	100	4.9	13	364
Hya	2.46 E+11	6.7	11.6	19	17	1.5	44.6	2.4	25	96
109P	1.29 E+11	5.9	8.2	29.7	28	2.8	23.4%	13.5	0.4	32571
65P	3.06 E+10	13.0	10.8	10	13	12	5.5%	3.7	1.3	2826
81P	2.09 E+10	10.2	11.4	13	17	17	3.8%	1.97	3.2	624
<b>103P</b>	<b>1.88 E+10</b>	<b>9.9</b>	<b>10.7</b>	<b>15</b>	<b>14</b>	<b>19</b>	<b>3.4%</b>	<b>0.57</b>	<b>33.9</b>	<b>17</b>
2P	1.33 E+10	3.1	4.8	98	64	27	2.4%	2.55	1.1	2321
9P	1.27 E+10	7.7	9.0	21	26	28	2.3%	2.75	0.98	2796
45P	7.95 E+09	3.5	7.5	55	40	45	1.4%	0.43	25.2	17
28P	3.58 E+09	4.5	3.2	100	133	100	0.6%	11.5	0.016	725892
26P	1.64 E+09	3.2	5.2	85	89	218	0.3%	1.47	0.44	3307
133P	1.81 E+08	0.2	1.4	----	280*	1978	0.32%	2.3	0.020	114796
107P	9.68 E+07	0.3	3.3	----	760*	3698	0.17%	1.65	0.021	79249

\*For comets 107P and 133P the definition of P-AGE(1,1) fails, so we give T-AGE(1,q) instead.

1139  
1140  
1141  
1142  
1143  
1144  
1145  
1146  
1147  
1148  
1149  
1150  
1151

1152  
 1153  
 1154  
 1155  
 1156  
 1157  
 1158  
 1159  
 1160  
 1161  
 1162  
 1163  
 1164  
 1165  
 1166  
 1167  
 1168  
 1169  
 1170  
 1171  
 1172  
 1173  
 1174  
 1175

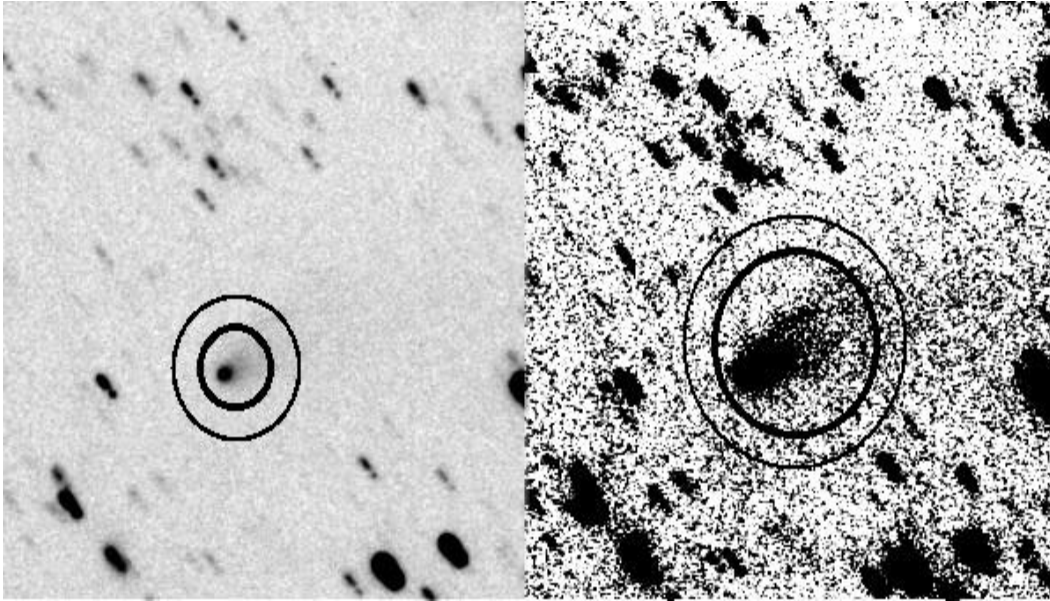


Figure 1.

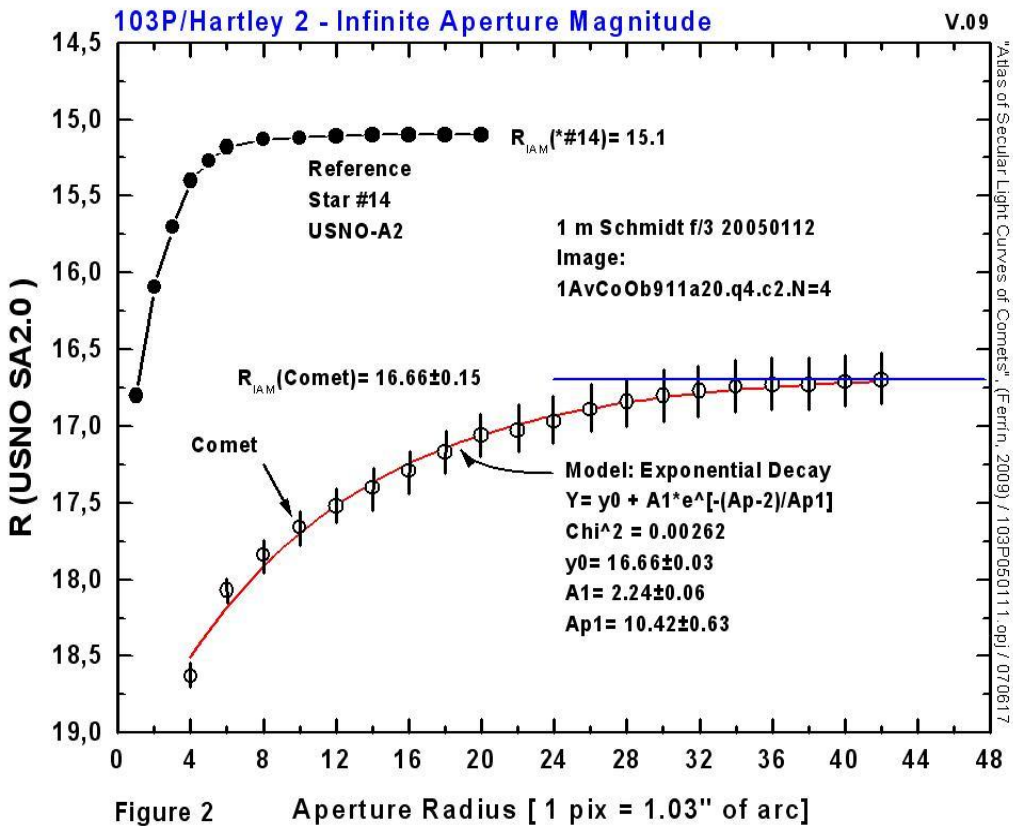


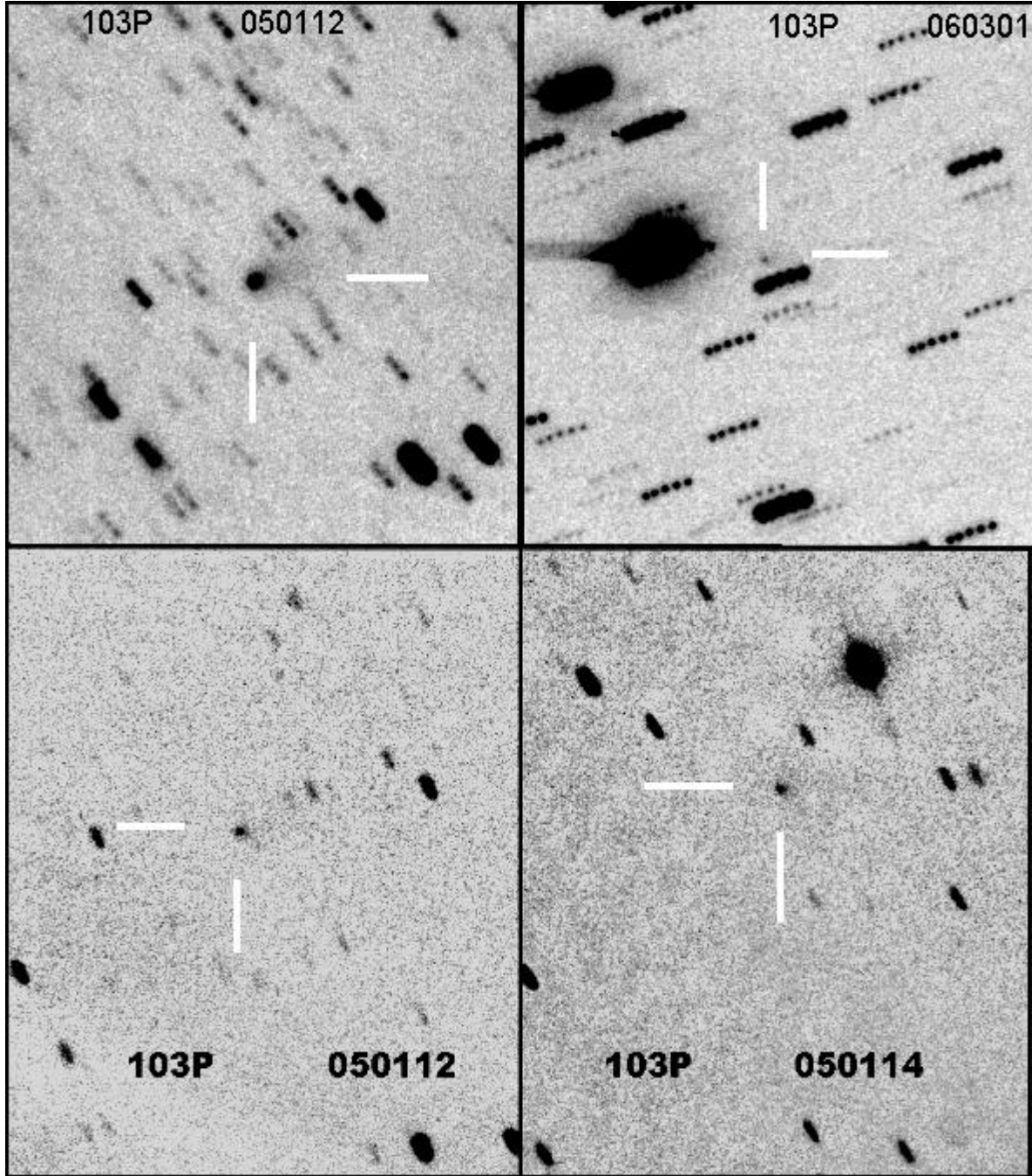
Figure 2

1176  
 1177

Figure 2



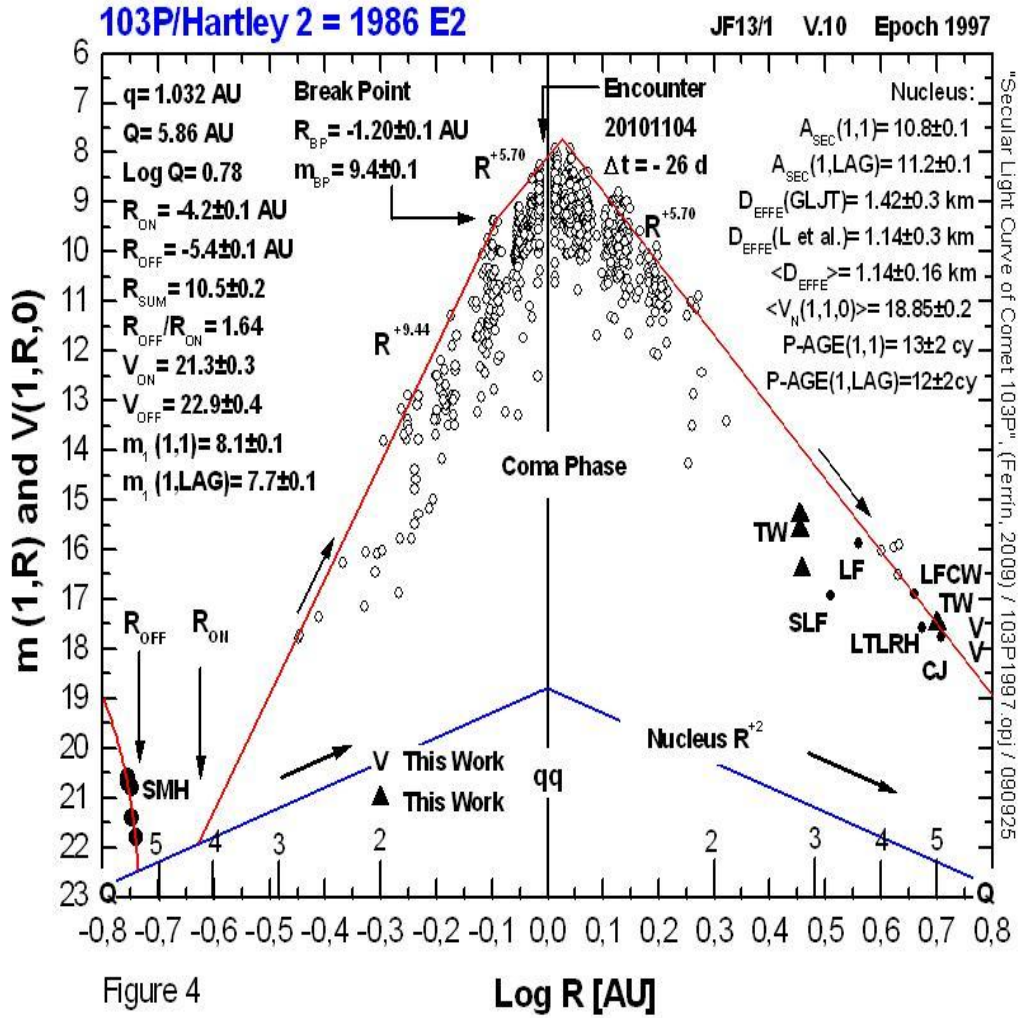
1178  
1179



1180  
1181  
1182  
1183  
1184  
1185  
1186  
1187  
1188  
1189  
1190  
1191  
1192

Figure 3

1193  
1194  
1195

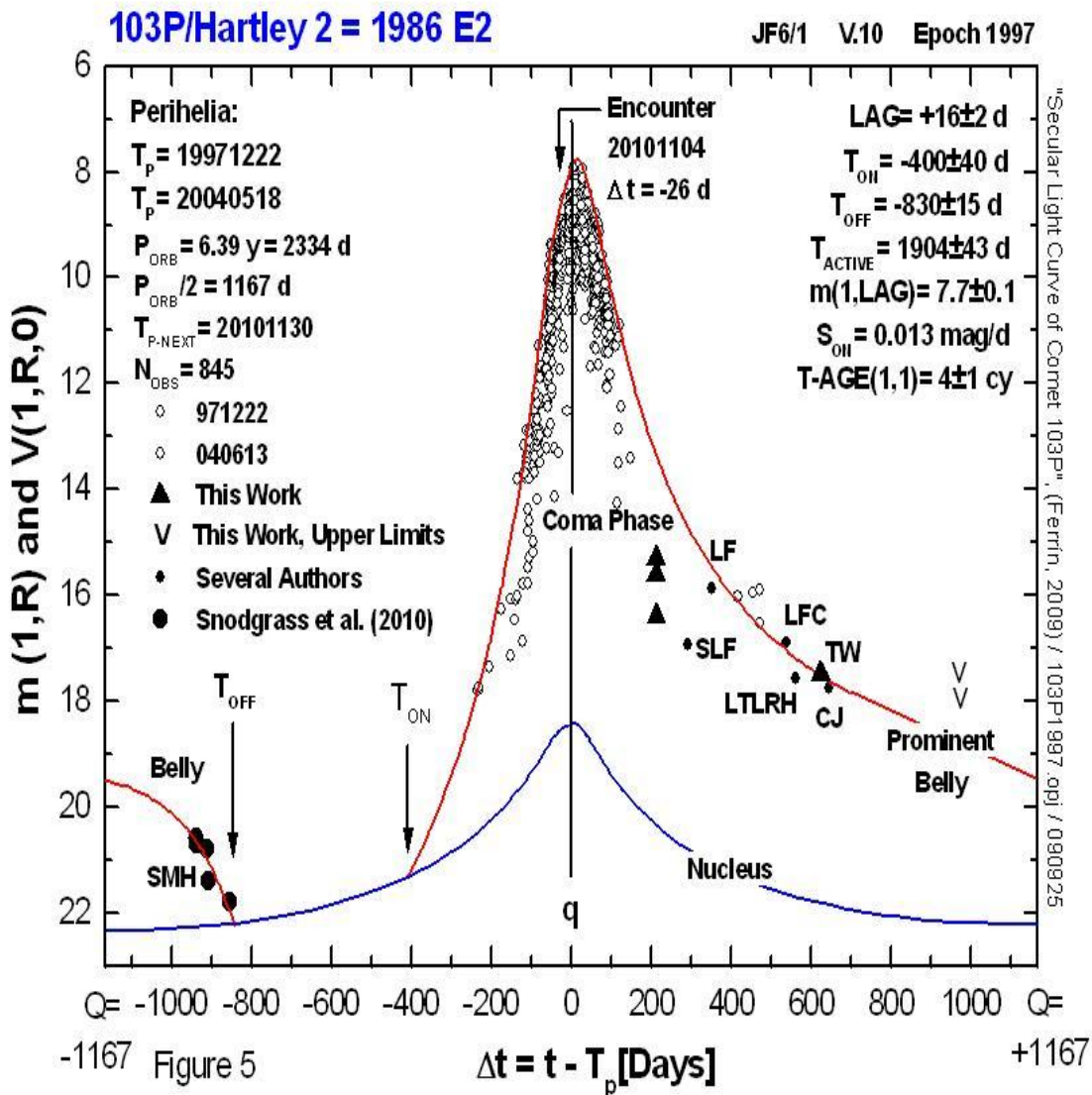


"Secular Light Curve of Comet 103P" (Ferrin, 2009) / 103P1997.qpl / 090925

1196  
1197  
1198  
1199  
1200  
1201  
1202  
1203  
1204  
1205  
1206  
1207  
1208  
1209  
1210

Figure 4

1211  
1212  
1213  
1214



1215  
1216  
1217  
1218  
1219  
1220  
1221  
1222  
1223  
1224  
1225  
1226  
1227

Figure 5

1228  
1229  
1230

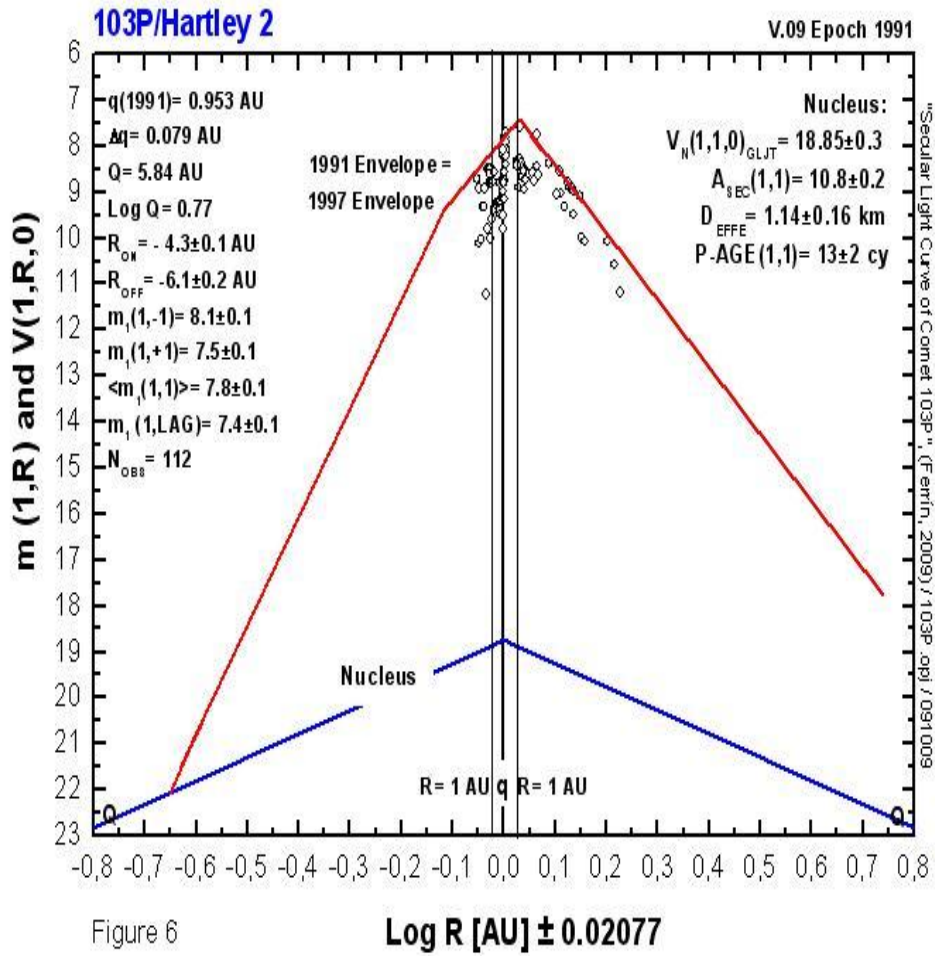
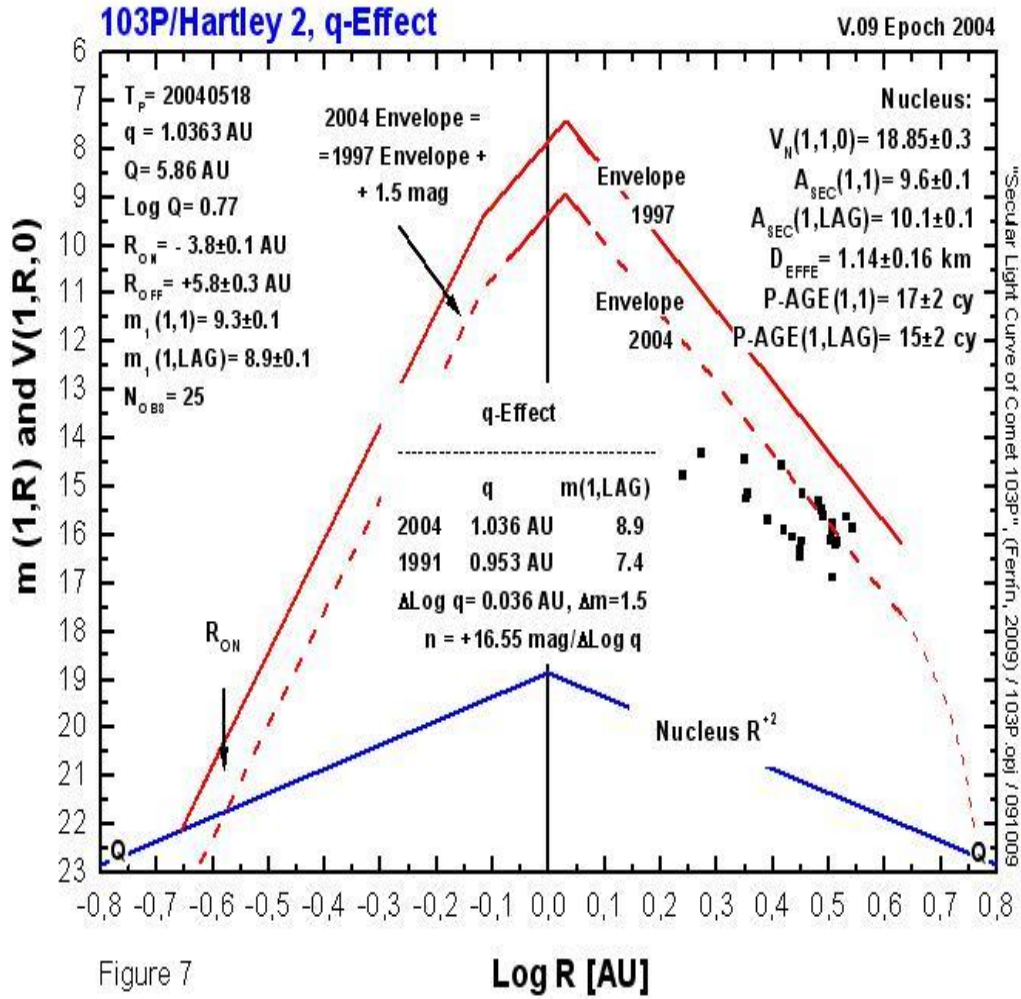


Figure 6

Figure 6

1231  
1232  
1233  
1234  
1235  
1236  
1237  
1238  
1239  
1240  
1241  
1242  
1243  
1244  
1245  
1246  
1247  
1248

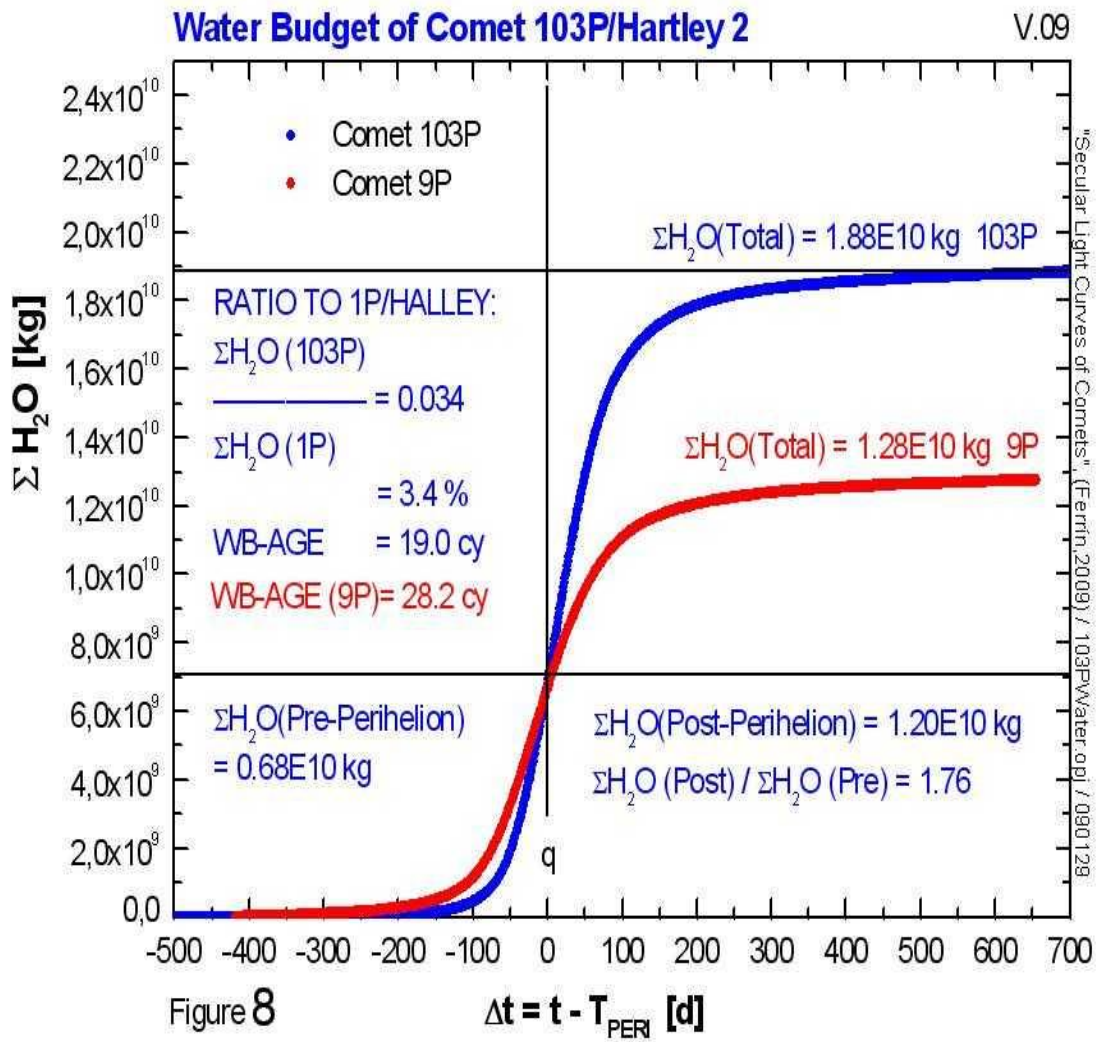
1249  
1250  
1251  
1252



1253  
1254  
1255  
1256  
1257  
1258  
1259  
1260  
1261  
1262  
1263  
1264  
1265  
1266  
1267  
1268

Figure 7

1269  
1270



1271  
1272  
1273  
1274  
1275  
1276  
1277  
1278  
1279  
1280  
1281  
1282  
1283  
1284  
1285  
1286  
1287

Figure 8

1288  
1289

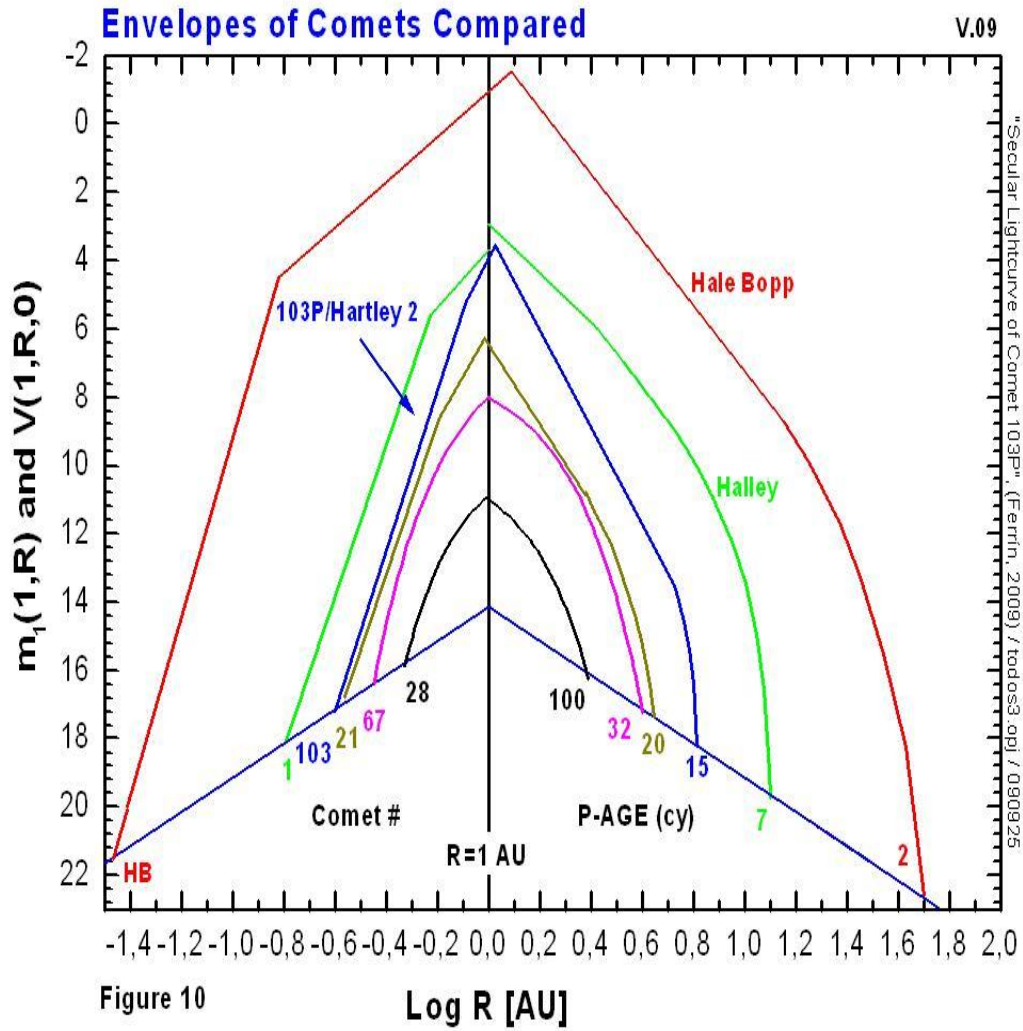
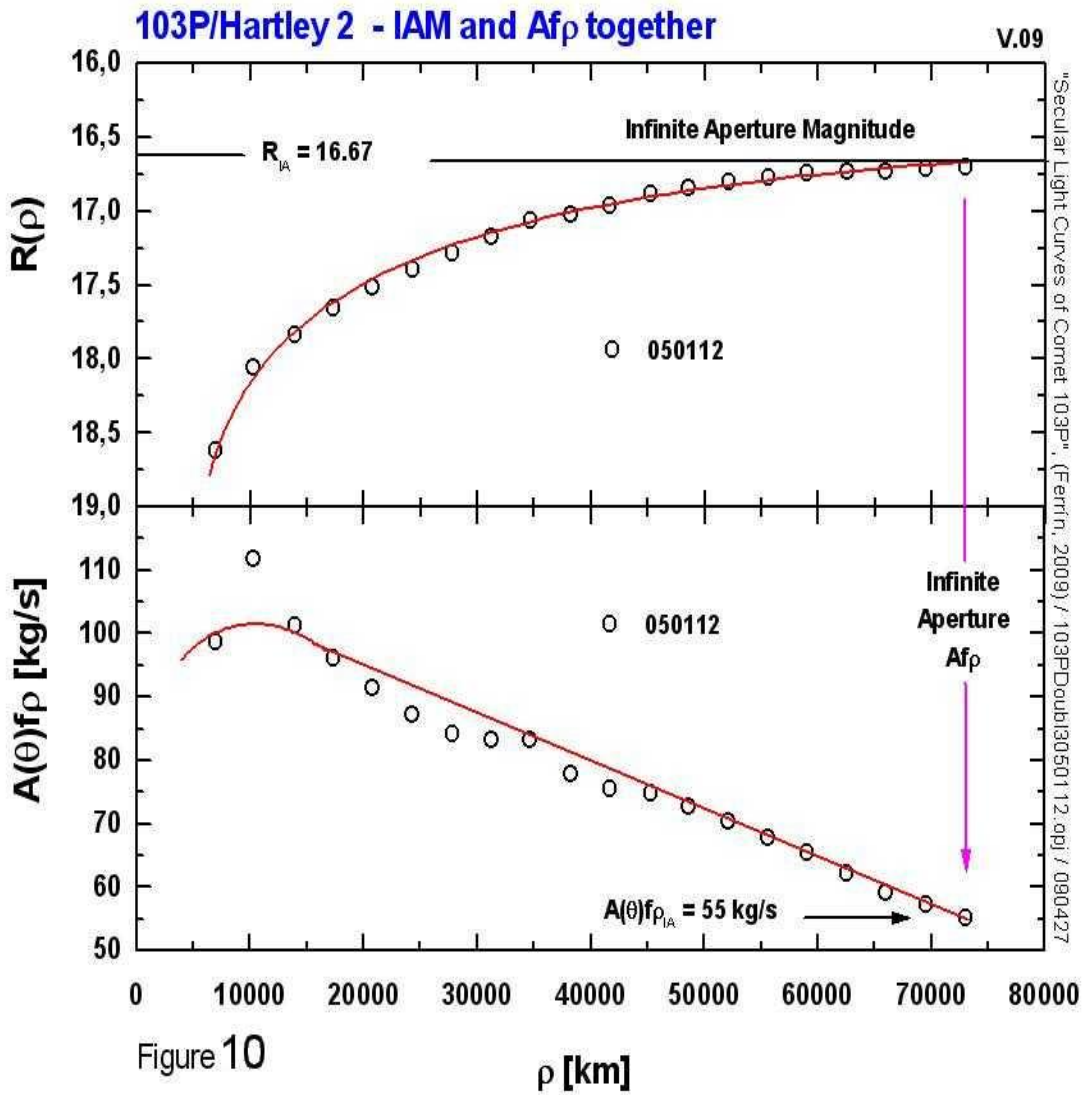


Figure 10

Figure 9

1290  
1291  
1292  
1293  
1294  
1295  
1296  
1297  
1298  
1299  
1300  
1301  
1302  
1303  
1304

1305  
1306

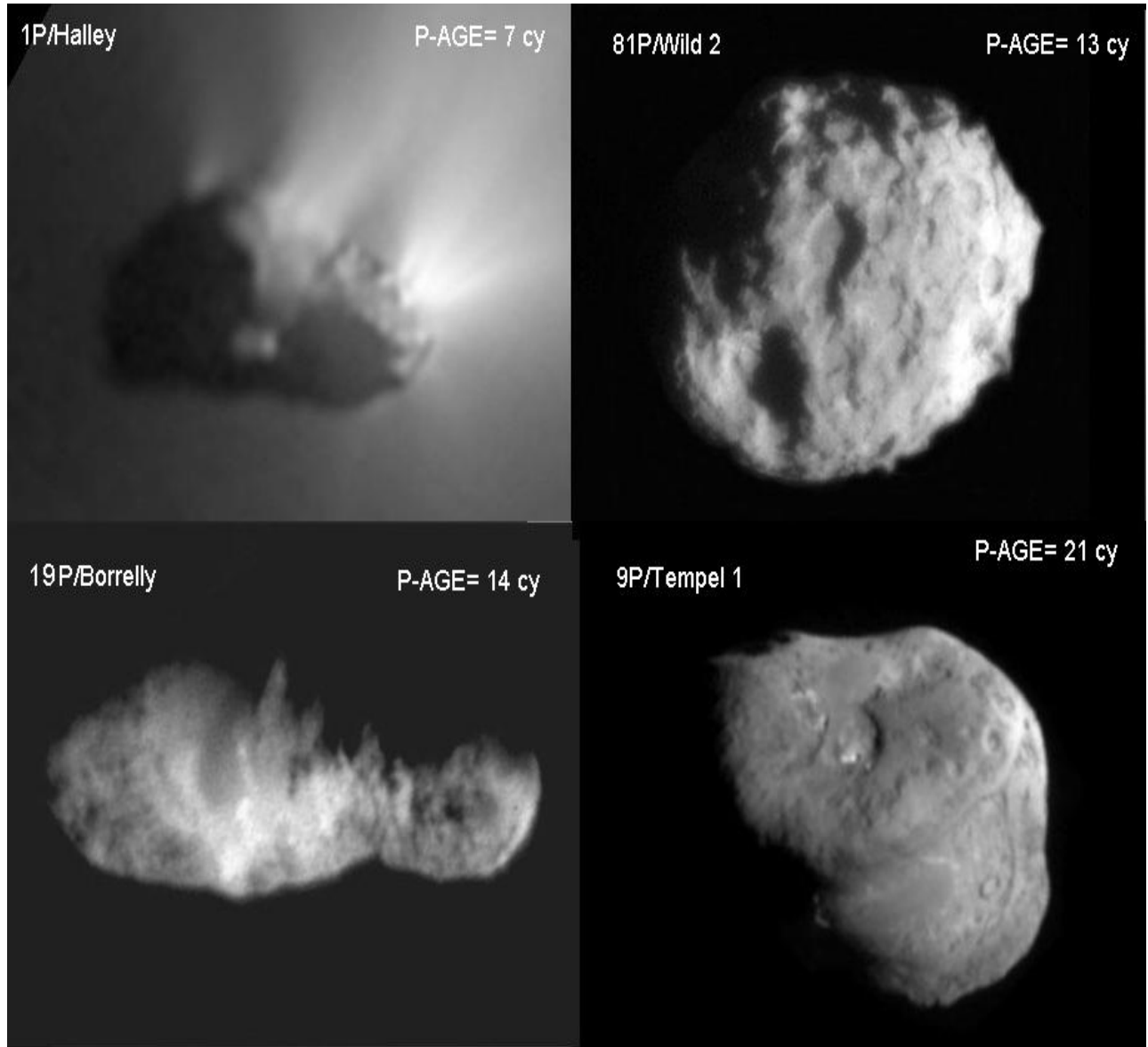


1307  
1308  
1309  
1310  
1311  
1312  
1313  
1314  
1315  
1316  
1317  
1318  
1319  
1320  
1321  
1322  
1323

Figure 10



1324  
1325



1326  
1327  
1328  
1329  
1330  
1331  
1332  
1333  
1334  
1335  
1336  
1337  
1338  
1339  
1340  
1341  
1342

Figure 11